GCAGS JOURNAL
A Publication of the Gulf Coast Association of Geological Societies
www.gcags.org

Comparison of Structural Styles Observed in Upper Eocene (Jackson Group) and Oligocene (Vicksburg Group) Strata within the Rio Grande and Houston Embayments Southwest and Northeast of the San Marcos Arch, Refugio and Calhoun Counties, South Texas Gulf Coast

Osareni C. Ogiesoba and Angela K. Eluwa

Bureau of Economic Geology, University of Texas at Austin, 10100 Burnet Rd., Austin, Texas 78759, U.S.A.

ABSTRACT

This paper presents structural styles associated with the upper Eocene (Jackson Group) and lower Oligocene (Vicksburg Group) located in the Rio Grande and Houston embayments southwest and northeast of the San Marcos Arch of the South Texas Gulf Coast, respectively. Previous studies that focused on the Rio Grande Embayment documented structural styles that include unusual coast-perpendicular faults, diapiric shale, and subbasins.

Present work involves mapping the structural styles in the Houston Embayment and comparing the deformational pattern in both basins using 3D seismic data from four different surveys. Two of the seismic surveys (surveys #1 and #2) are located in Refugio County in the Rio Grande Embayment. The other two are located in the Houston Embayment—one (survey #3) within Calhoun County and the other (survey #4) straddling Calhoun and Jackson counties and Matagorda Bay. Methods of investigation consist of seismic interpretation, 3D visualization, and seismic-attribute extraction.

Our map at the top of the Vicksburg in the vicinity of the San Marcos Arch shows that: (1) although the prevailing mechanism of deformation during the deposition of the Eocene (Jackson Group) and Oligocene (Vicksburg Group) in the Rio Grande and Houston embayments was extensional tectonics, stratal deformational patterns are different in each basin; (2) in the Rio Grande Embayment, the dominant structural styles are mostly coast-orthogonal faults and shale ridges, prominent northeast-southwest-southeast trending curvilinear anticlines, and coast-parallel synthetic and antithetic faults; whereas in the Houston Embayment, the dominant structural styles consist of coast-parallel synthetic growth faults and shale diapirs; (3) the Houston Embayment is about 3050 m (10,015 ft) deeper than the Rio Grande Embayment; (4) the remnant erosional anticlinal structure within the Houston Embayment constitutes a potential hydrocarbon prospect; and (5) the diapiric structure along COCORP line TX4 in the Houston Embayment is interpreted to be composed mostly of overpressured shale.

INTRODUCTION

Although much work has been conducted in the Rio Grande and Houston embayments (e.g., Halbouty, 1966; Galloway et al., 1982; Culotta et al., 1992; Galloway et al., 2000; Ogiesoba and Hammes, 2012; Ogiesoba and Hernandez, 2015), a comparison of structural styles within these basins in the vicinity (southwest and northeast) of the San Marcos Arch has yet to be published. The Rio Grande Embayment is bordered to the southwest by the northwest-trending frontal folds of a Late Mesozoic–Cenozoic fold-thrust belt in Mexico (Sierra Madre Oriental) and to the northeast by the San Marcos Arch. The Houston Embayment is bordered to the northeast by the Belton High and the Sabine Arch (Halbouty, 1966), with the San Marcos Arch forming its southwestern boundary. Both the Houston and Rio Grande embayments are bordered to the northwest by the Ouachita Tectonic Belt (Halbouty, 1966). Because of tectonic activities associated with the intermittent motion of the San Marcos and Sabine arches during the waning phases of the Laramide compression, and because of the onset of volcanism and magmatism in the early Oligocene during deposition of the Vicksburg Group (continuing into the Miocene and ending at about 17 Ma) (Henry and

Manuscript received March 20, 2019; revised manuscript received June 14, 2019; manuscript accepted August 16, 2019.

GCAGS Journal, v. 8 (2019), p. 170–190.
DOI: pending

McDowell, 1986), the two arches have played a key role in the control of sediment deposition and deformation in the Rio Grande and Houston embayments.

Angular unconformity and thinning of stratigraphic units over these arches indicate that both the San Marcos and Sabine arches were intermittently positive areas in the Late Cretaceous and early Paleogene (Murray, 1961). A second Paleocene episode of motion between the Sabine Arch and adjacent basins is marked by thickening of the Wilcox Group delta-plain sediments in the East Texas Basin and thinning across the arch (Laubach and Jackson, 1990). A Halbouty (1966) diagrammatic geologic section showed that the Vicksburg Group thins considerably (~165 m [~540 ft]) over the San Marcos Arch compared to its thickness in the Rio Grande (~680 m [~2240 ft]) and Houston (~890 m [~2920 ft]) embayments, which suggests that the arch was in motion during the Oligocene. According to Halbouty (1966), the San Marcos Arch played a key role in influencing the stratigraphic and structural attitudes of strata in adjacent basins from the Jurassic to early Neogene.

Objective

Three previously published works played very pertinent roles in defining the objectives of this current project. Culotta et al. (1992) discussed the results of the Consortium for Continental Reflection Profiling (COCORP) seismic survey along the San Marcos Arch. The survey line consists of three line segments (TX4, TX5, and TX6) covering a distance of 250 km (~156 mi) from Port Lavaca on the central Texas coast to the southeastern side of the Llano Uplift (Fig. 1A). Based on the authors' interpretation of this line (Fig. 1B), the Vicksburg and Jackson groups at the extreme southeastern end of the survey have not been penetrated by any well. Well 11, located at the southeastern end of TX4, was drilled to depths of about 2300 m (~7550 ft) but did not encounter the Vicksburg, suggesting that the strata are located at a depth greater than 2300 m (7550 ft). In fact, it appears that the Vicksburg and Jackson were faulted down thousands of meters by a couple of major synthetic and antithetic faults (Fig. 1B). Thus, the depths at which the tops of these strata occur in the Houston Embayment at this location are not certain. Furthermore, directly below the total depth of well 11, Culotta et al. (1992) tentatively interpreted a diapiric structure (Fig. 1B), suggesting doubts about the actual composition of the structure; whether it is composed of shale or salt is yet to be resolved. The remaining wells to the northwest penetrated the top and base of the Vicksburg and Jackson, with the exception of wells 9 and 10, which penetrated only the top of the Vicksburg. At the southeastern end of TX6, the authors interpreted the outline of the Luling Uplift (Fig. 1B), a Precambrian rock that is closely associated with the San Marcos Arch (Fig. 1A).

The second influential paper is Coleman and Galloway (1990), which discusses oil and gas field distribution within the Vicksburg in the Rio Grande and Houston embayments and in the vicinity of the San Marcos Arch (Fig. 2). In Figure 2, we have superimposed the COCORP line (TX4, TX5, and TX6 [bold magenta line segments]). As shown, the southeastern part of TX4 is completely on the downthrown side of fault B, where information about the Vicksburg is scanty—no oil or gas field has been identified in this area of Calhoun County in the Houston Embayment. Thus, the area needs further investigation and constitutes part of our study area. The third influential paper, Ogiesoba and Hernandez (2015), shows that, in addition to synthetic and antithetic growth faults, the dominant structural features in the Rio Grande in the vicinity of the San Marcos Arch are coast-orthogonal shale ridges, subbasins, and coast-orthogonal faults.

Based on the foregoing discussion, the objectives of this project are to (1) determine the lithological composition of the diapiric structure that sits directly below well 11 along line TX4, (2) determine the similarity between the deformational pattern in the Vicksburg Group within the Rio Grande and the Houston embayments in the vicinity of the San Marcos Arch, and (3) identify any structurally and stratigraphically trapped hydrocarbon play within the Vicksburg in the Houston Embayment. Our current effort builds on the results of Ogiesoba and Hernandez (2015) by extending the previous interpretation into Victoria County using additional 3D seismic volume and by mapping the top of the Vicksburg in the Houston Embayment in the vicinity of the San Marcos Arch.

LOCATION AND GEOLOGY OF STUDY AREA

The study area is located partly in the Rio Grande Embayment, straddling Refugio and Victoria counties, and partly in the Houston Embayment, straddling Calhoun and Jackson counties and Matagorda Bay about 30–40 km (~19–25 mi) northeast of the San Marcos Arch axis (Fig. 3). The stratigraphic section of interest stretches from the Eocene Jackson Group to the late Oligocene Anahuac Shale, with particular emphasis on the Vicksburg Group (Fig. 3). In the Rio Grande Embayment southwest of the San Marcos Arch axis, stratal thicknesses (isopachs) are thinner than in the Houston Embayment northeast of the arch. In fact, although the top of the Vicksburg has not been penetrated by any well in our study area in the Houston Embayment, the Frio Formation is up to 2440 m (~8000 ft) thick at some locations, such as in the Damstrom #1 well in the Appling Field in the Carancahua Bay area.

DATABASE

The database consists of four 3D seismic surveys, #1 through #4. The first two surveys are located in the Rio Grande Embayment. Survey #1 consists of a 25 x 25 m (~80 x 80 ft) stacking-bin size covering an area of ~125 km^2 (~48 mi^2), with a sampling interval of 4 ms. Survey #2, directly southeast of survey #1, has a 25 x 25 m (~80 x 80 ft) stacking-bin size with an area of ~260 km^2 (~104 mi^2). The sampling interval is also 4 ms. Both surveys have a record length of ~6 s each. Surveys #3 and #4 are located in the Houston Embayment northeast of the San Marcos Arch (Fig. 4). Survey #3 is located entirely in Calhoun County and covers an area of 130 km^2 (~50 mi^2). It has a stacking-bin size of 34 x 34 m (~110 x 110 ft), with a sampling interval of 2 ms and a record length of 6 s. Survey #4 straddles Calhoun and Jackson counties and Matagorda Bay, covering an area of ~196 km^2 (~76 mi^2). It has a stacking-bin size of 34 x 34 m (~110 x 110 ft), with a 4 ms sampling interval and a record length of 6 s.

In the Houston Embayment, although more than 100 wells have been drilled in the area covered by surveys #3 and #4, none penetrated the top of the Vicksburg. The average depth of these wells ranges from ~2135–2740 m (~7000–9000 ft), although a few have been drilled up to 3960–5200 m (~13,000–17,000 ft). In survey #1, located in the Rio Grande Embayment, only one available well (well J, Fig. 4) has penetrated the top of the Vicksburg (at ~1990 m [~6520 ft]) down to near the base of the Eocene Jackson Shale. The total depth of well J is ~3554 m (~11,660 ft). Wireline-log suites consist of sonic, gamma ray, resistivity, and spontaneous potential curves.

METHODS

The first step, beginning with survey #1 in the Rio Grande Embayment, was to tie the wells to the seismic data. We identified the tops and bases of the Oligocene (Anahuac, Vicksburg, and Frio) and Eocene (Jackson Group). These tops were interpreted throughout the entire survey and across the down-to-the-southeast synthetic faults into survey #2 (Fig. 5). Five surfaces plus two detachment surfaces (detachment surfaces 1 and 2,

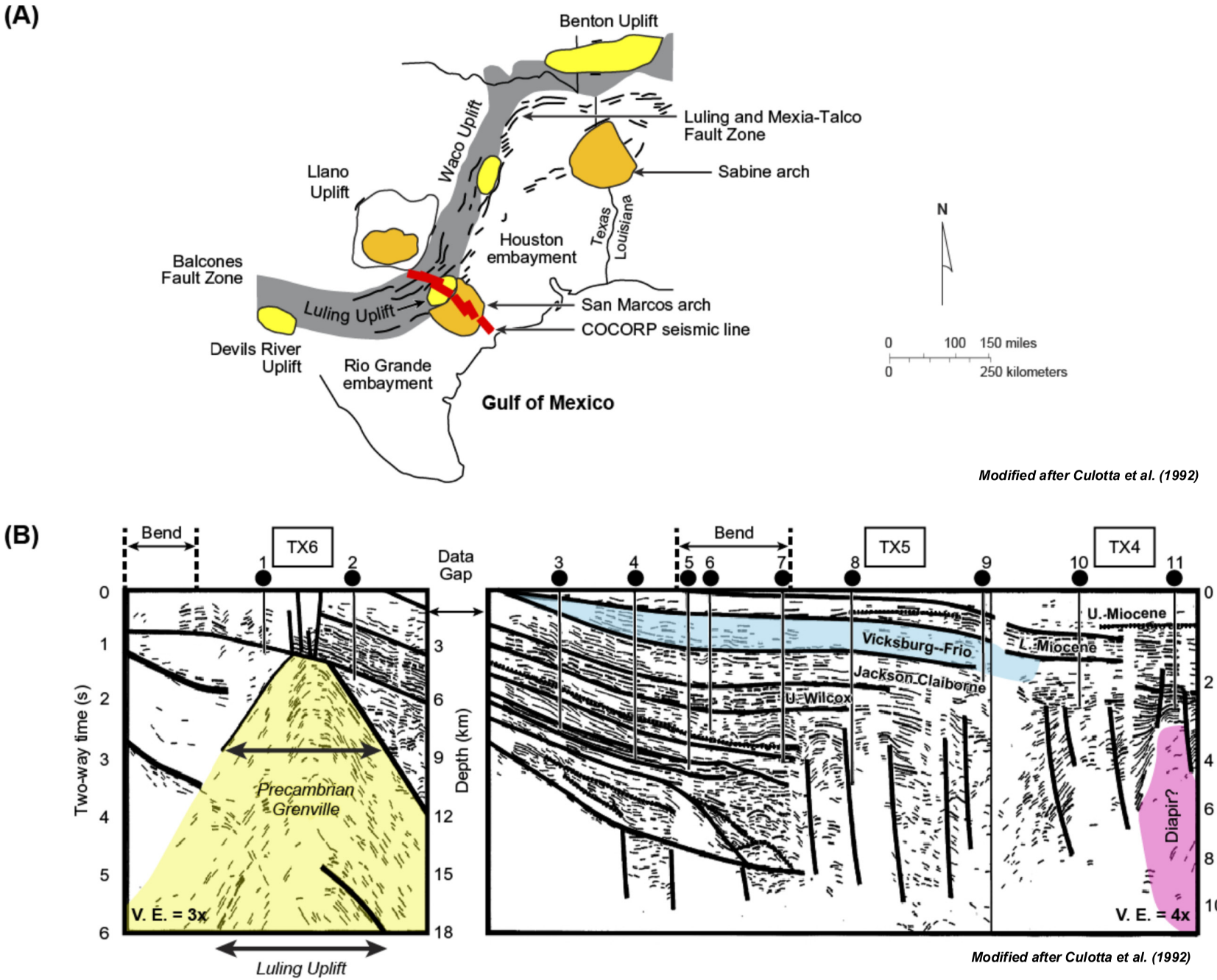

Figure 1. (A) Map of South Texas showing Precambrian arches and uplifts, and location of COCORP seismic line (modified after Culotta et al., 1992). (B) COCORP's minimal interpretation of line segments TX4, TX5, and TX6 (modified after Culotta et al., 1992). 1 km = ~0.62 mi.

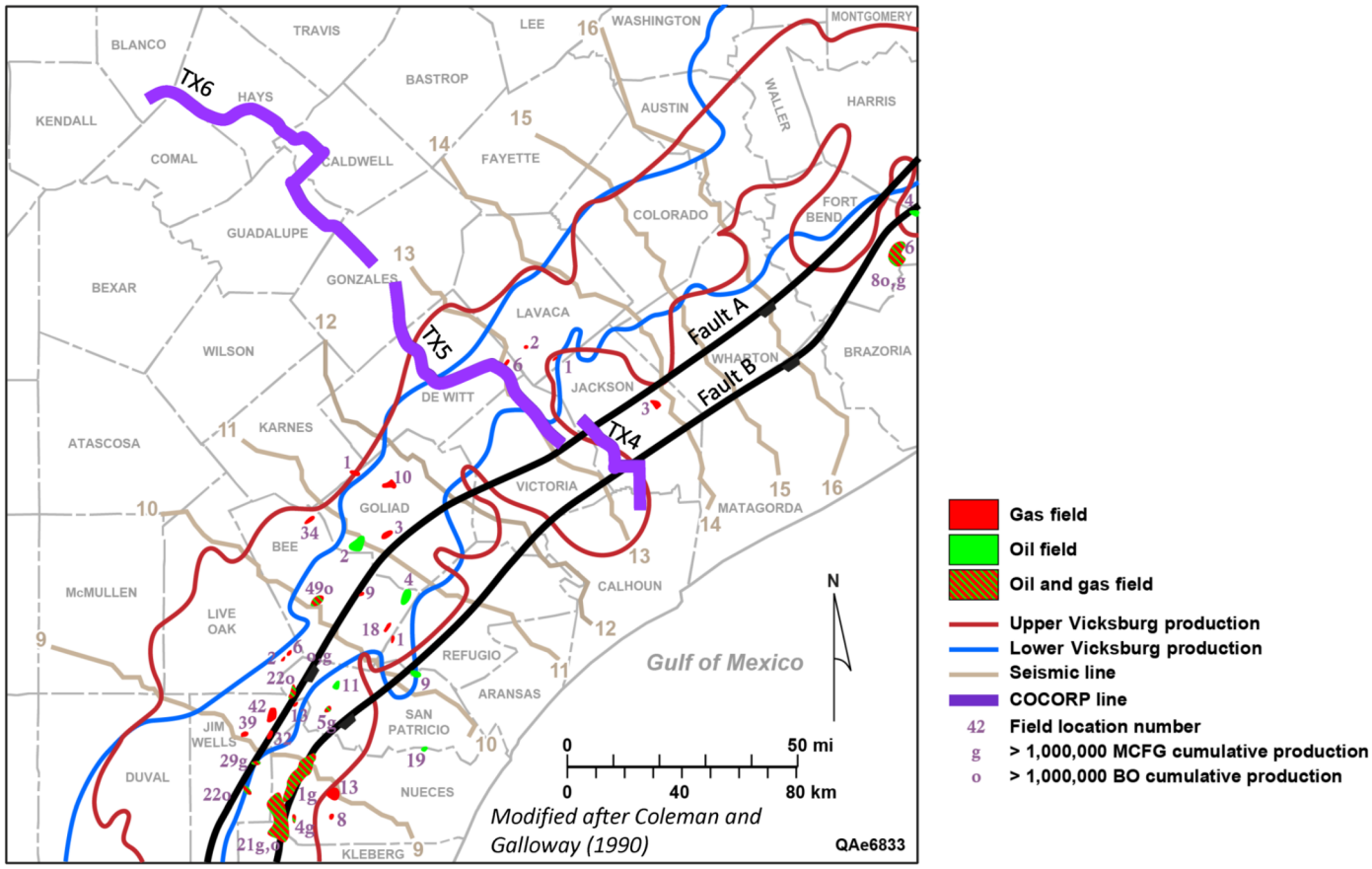

Figure 2. Distribution of oil and gas fields of San Marcos Arch area with superimposed COCORP TX4, TX5, and TX6 line segments (magenta color) (modified after Coleman and Galloway, 1990). Wells are numbered 1 through 11.

Fig. 5) were interpreted in survey #1. Detachment surface 1 (cyan surface) occurs just below the base of the Jackson, while detachment surface 2 (yellow surface) occurs at much greater depth. These two surfaces were not identified in the other three surveys. Although five surfaces were interpreted, because the focus is on the Vicksburg, only the map at the top of the Vicksburg is discussed. In surveys #3 and #4 in the Houston Embayment, because the Vicksburg and the Jackson are located at much deeper depths than those in the Rio Grande Embayment, none of the available wells has penetrated the tops of these stratigraphic units, making interpretation of the tops of these two units difficult. However, after tying one of the deep wells (well K, Fig. 4) to seismic data in survey #4, we interpreted the top of the Vicksburg as a major detachment surface onto which fault A soles out. It appears as an unconformity surface at the base of the lower Frio (seismic line B–B', Fig. 6). The base of well K is in shale at a total depth of 4500 m (14,780 ft). The top of the Vicksburg is characterized as a surface onto which the lower Frio strata structurally rotated. In some cases, it truncates underlying beds and also serves as a decollement surface for lower Frio shale-rich strata (dashed black arrow, Figs. 6, 7, and 8).

In survey #3, difficulty in recognizing the top of the Vicksburg is compounded by severe structural deformation. The closer one approaches the San Marcos Arch from the northeast direction, the greater the structural deformation. However, by carefully comparing parallel seismic lines C–C' and D–D', E–E' and F–F', and F–F' and H–H' from both surveys #3 and #4, we interpret the top of the Vicksburg in survey #3 (Figs. 7, 8, and 9). In this area, the top of the Vicksburg also appears as an unconformity (yellow surface, Fig. 6A) onto which lower Frio sediments downlap (red arrows, Fig. 9A). However, because of the limited areal extent of this surface, we mapped the green surface (Fig. 9A). Having identified the top of the Vicksburg in both surveys, we also interpreted the top and base of the Anahuac Shale. The top and base of the Jackson Shale were not interpreted because of the absence of penetrations.

RESULTS

This section presents the map at the top of the Vicksburg in surveys #1 to #4. Only the dominant structural features in each survey are discussed, starting with survey #1 in the Rio Grande Embayment.

Rio Grande Embayment: Survey #1

The main structural elements in this acreage are the down-to-the-basin, coast-parallel, synthetic growth faults (Figs. 5 and 9). Although the map at the top of the Vicksburg in this acreage is of small areal extent, being ~125 km^2 (~48 mi^2), it nevertheless presents some unique structural features that include a curvilinear anticlinal structure. The anticline at first trends northeast-southwest, then to the southeast, where it becomes a coast-orthogonal structure (Fig. 10). It is broken into two unequal halves by a down-to-the-southeast, crestal, synthetic fault (fault CV). The fault is also curvilinear, trending along the length of the anticline from northeast to southwest, then to the southeast, where it assumes a coast-orthogonal attitude (Fig. 10). The fault cuts well J at the top of the Vicksburg (Figs. 5 and 10). In addition to fault CV, a combination of three other faults—faults CV–

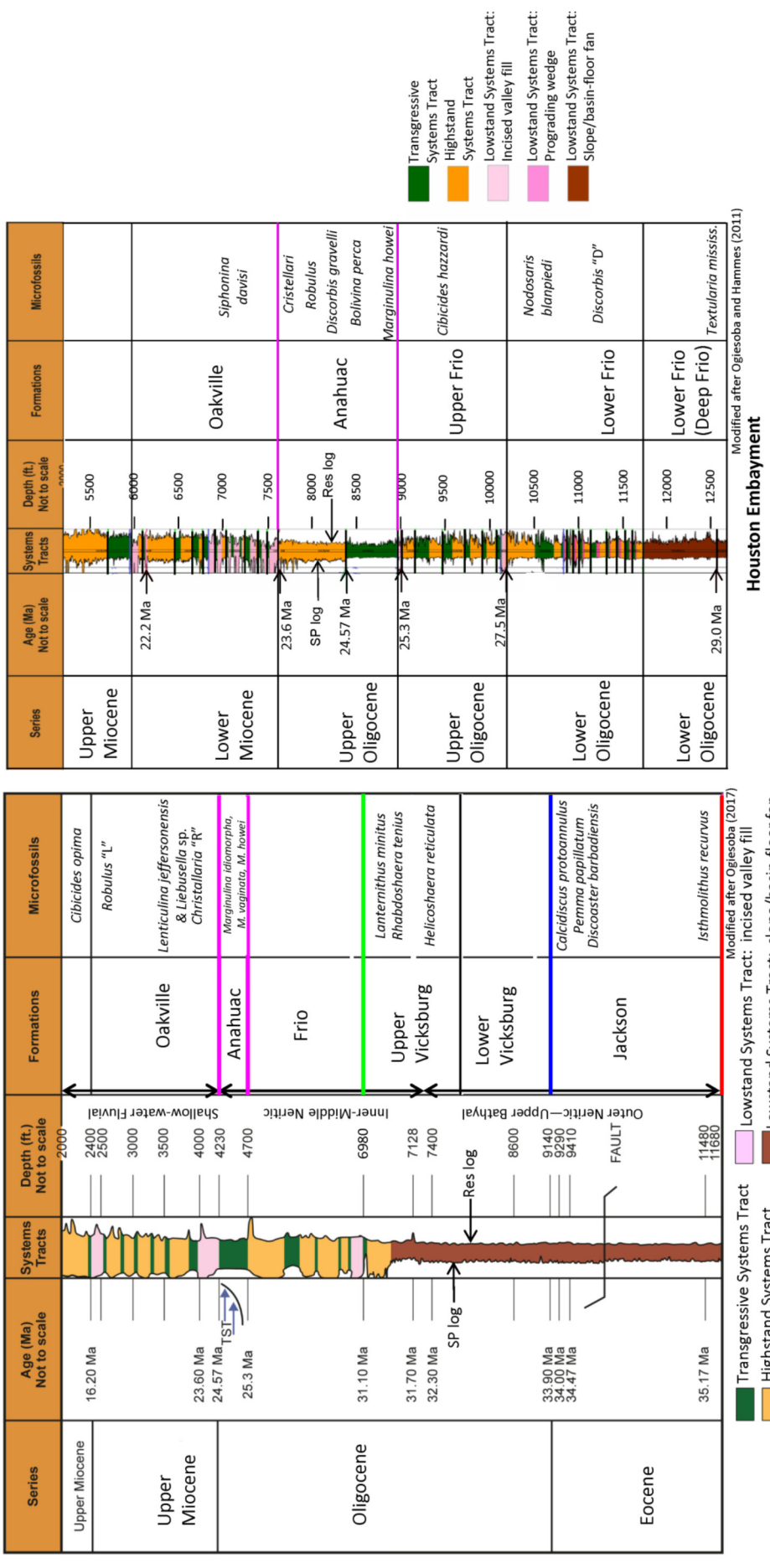

Figure 3. Stratigraphic columns from (A) southwest side of San Marcos Arch in the Rio Grande Embayment showing interpreted horizons—top and base Anahuac (magenta), top Vicksburg (green), and top Jackson (deep blue). (B) Northeast side of San Marcos Arch in the Houston Embayment showing only top and base Anahuac (magenta); top Vicksburg and top Jackson are not seen. 1000 ft = ~304.8 m.

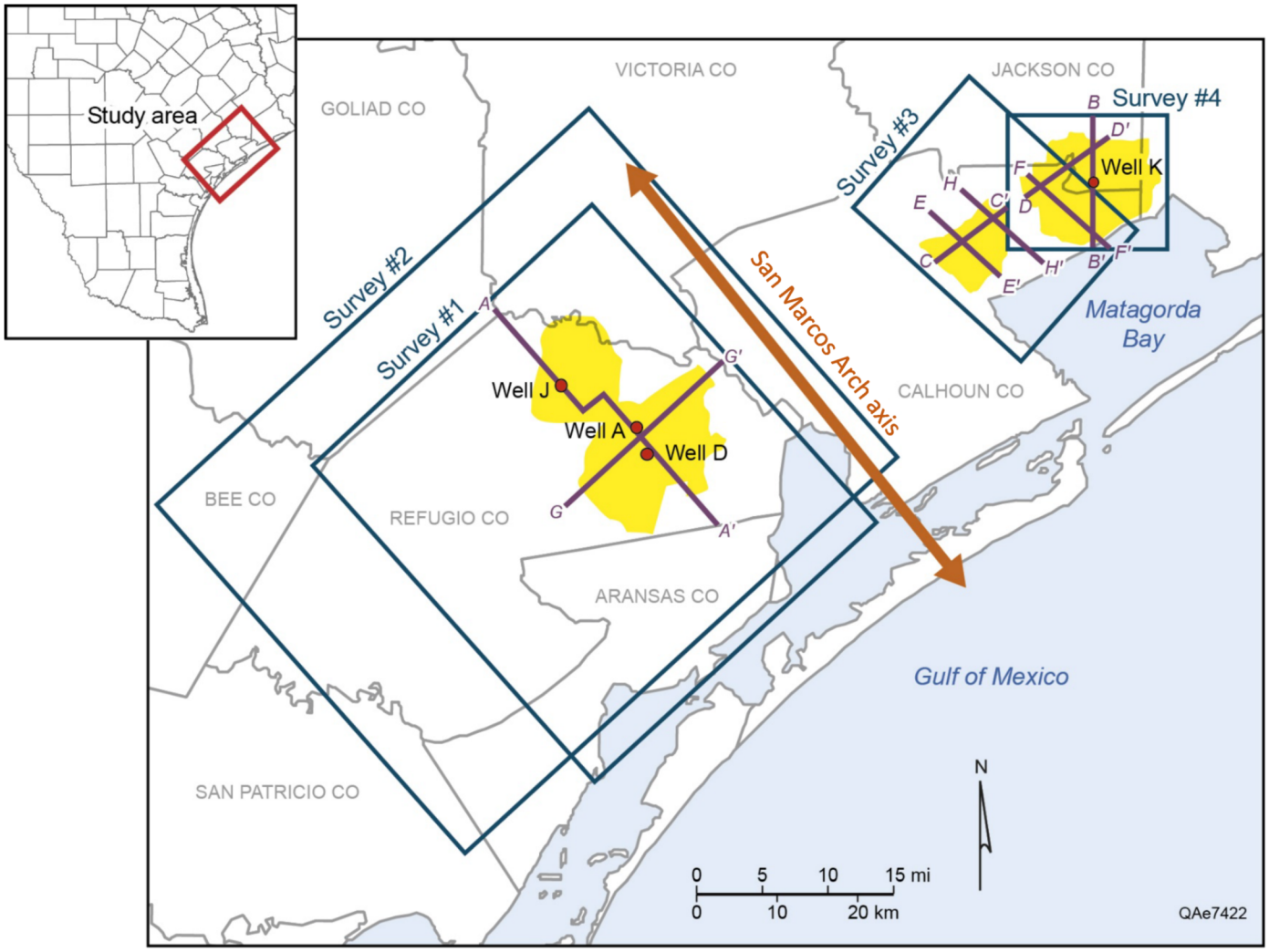

Figure 4. (A) Map of South Texas showing study area (red rectangle). (B) Enlarged version of red rectangle showing Refugio, Calhoun, Victoria, and Jackson counties; Matagorda Bay; and San Marcos Arch axis. Blue rectangular outlines = 3D survey boundaries for surveys #1 to #4; yellow outlines = area where seismic data is available in each survey; solid red circles = well locations; magenta lines = seismic lines discussed in text.

1, CV–2, and CV–3—separate the northwestern part of the anticline, which is also curvilinear (magenta arrow), from the southeastern part (red arrow) (Fig. 10). Apart from fault CV, all other faults are coast-parallel synthetic faults.

Although the mechanism responsible for the curvilinear anticline is not clear, deposition occurred during extension (Galloway et al., 2000).

Rio Grande Embayment: Survey #2

The main structural elements in survey #2 consist of coast-orthogonal faults, subbasins, shale ridges, and coast-parallel synthetic and antithetic faults. The entire survey #2 area is located in a minibasin that is bound on the northeast by the San Marcos Arch, being ~10 km (~6 mi) from the arch. The top of the Vicksburg interpreted surface in this survey is separated from the top of the Vicksburg surface in survey #1 by a down-to-the-southeast synthetic fault HB (Fig. 5). The map in survey #2 illustrates four alternating coast-orthogonal shale ridges (SD 1 to SD 4) and subbasins (SB 1 to SB 4) (Fig. 11). Within the subbasins are coast-parallel synthetic faults located in the northern part and coast-parallel antithetic faults located in the southern part. At the flanks of the shale ridges, the coast-parallel synthetic and antithetic faults merge to form three coast-orthogonal, down-to-the-southwest faults (Ogiesoba and Hernandez, 2015) (Fig. 11). Along seismic line G–G' (Fig. 12), alternating shale diapirs and subbasins are highly pronounced.

Houston Embayment: Survey #3

The dominant structural elements in this survey consist of coast-parallel synthetic faults and shale ridges. The survey is located on the northeast side of the San Marcos Arch, ~30 km (~19 mi) from its axis. Because of the complex faulting and shale diapirism prevalent in this acreage, the mappable area of the top of the Vicksburg is very limited, particularly in the southeastern part. To gain better insights into structural styles in this area, we mapped another surface (green surface) ~300 ms deeper than the top of the Vicksburg (yellow surface) (Fig. 7A). This green surface covers a larger area and also addresses the structural picture in the southeastern part of the area. The map shows that although there are some minor coast-orthogonal faults, the main structural elements are down-to-the-southeast synthetic faults and shale diapirs (Figs. 7, 8, and 13A). Along the fault plane of one of the major synthetic faults, folded fault blocks (bold, dashed red arrow) are rafted downslope basinward, having

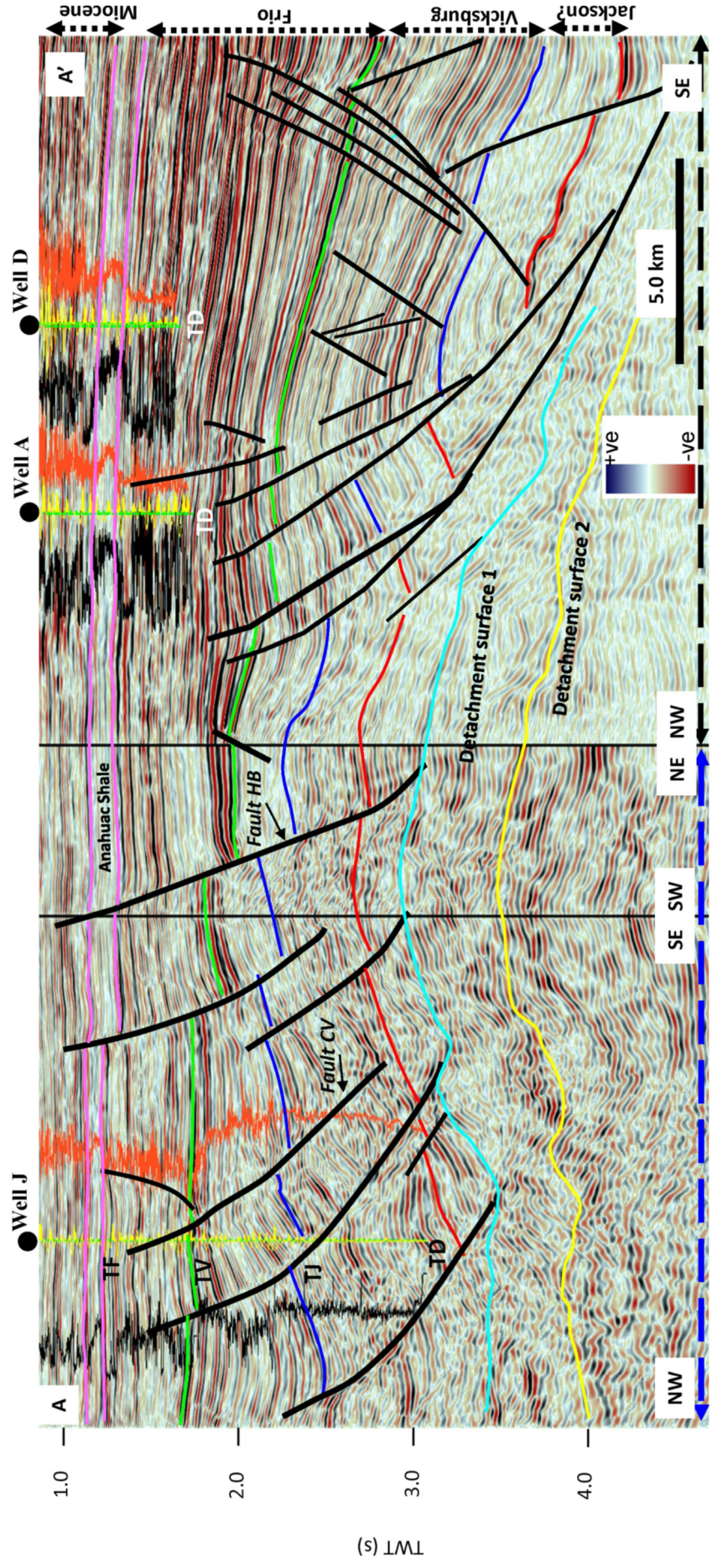

Figure 5. Seismic line A–A' through wells J, A, and D. Displayed log curves are gamma ray (black) and sonic (red) logs. Sonic log deflection to right = increasing sonic values (i.e., decreasing velocity); deflection to left = decreasing sonic values (i.e., increasing velocity). Note: sonic scaling is reversed from standard scaling. Deflection of gamma ray log to right = increasing shale content; deflection to left = decreasing shale content. Yellow curve = synthetic trace. Double-headed, dashed blue arrow = seismic data from survey #1; double-headed, dashed black arrow = seismic data from survey #2. 5 km = ~3.1 mi.

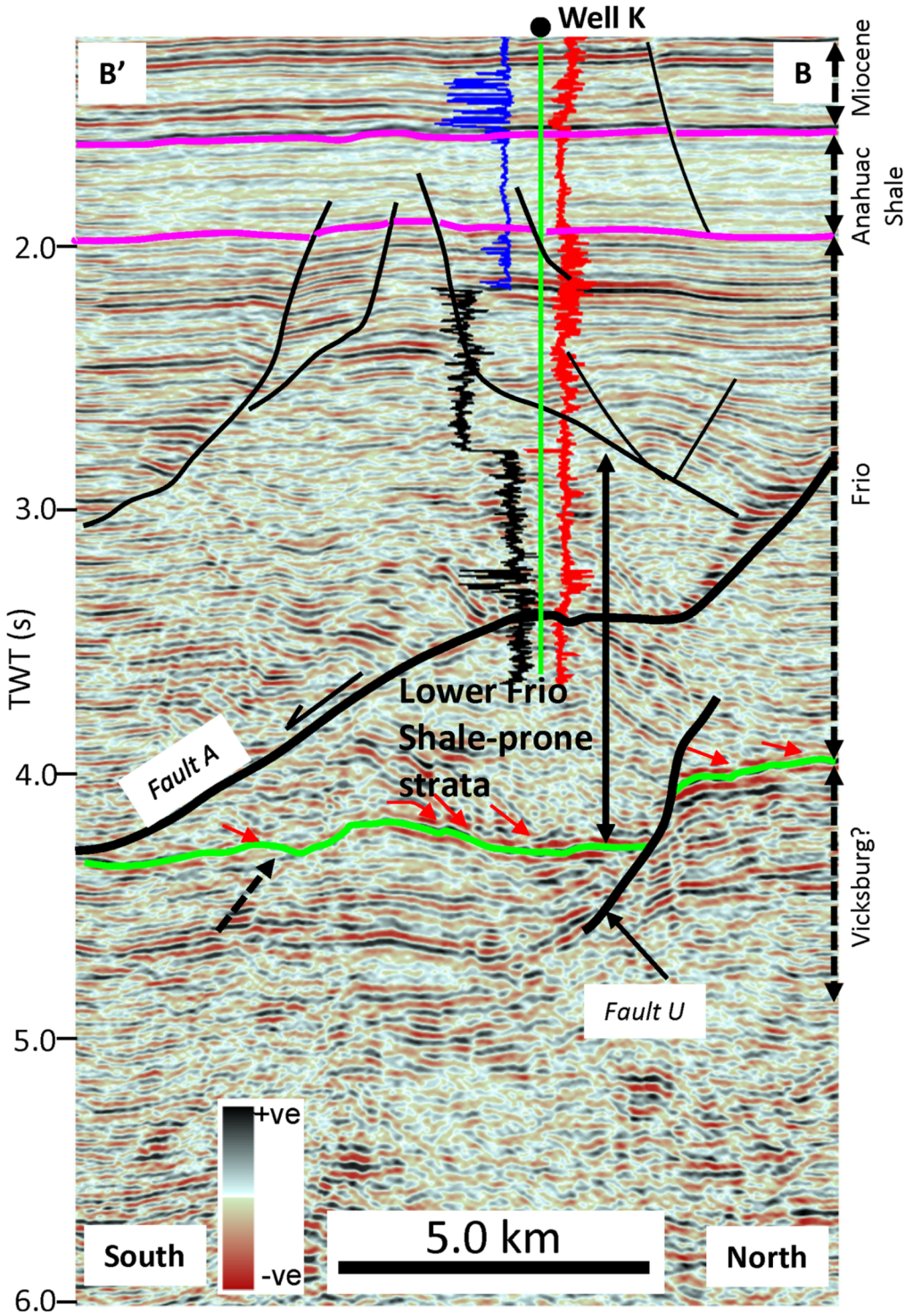

Figure 6. Seismic line B–B' through well K showing seismic data and interpreted horizons from survey #4. Top and base Anahuac Shale shown in magenta color; top of Vicksburg Formation shown in green; and small red arrows indicate direction of downlap of lower Frio strata on top Vicksburg surface. Blue log curve = spontaneous potential log; black log curve = gamma ray log; and red log curve = resistivity log. Upper Frio Formation is sand dominated, and lower Frio Formation is shale dominated. Note unconformable nature of Vicksburg surface (dashed black arrow). 5 km = ~3.1 mi.

travelled 1.0 km (~0.62 mi) (Fig. 8A). The minor coast-orthogonal faults are antithetic faults whose northeast arms extend northward to form coast-orthogonal faults (Fig. 13A). These antithetic faults occur at the flank of a shale-cored anticline. Although seismic data in the northern part of survey #3 is of fair to poor quality, based on well information, we confirmed the presence of a shale ridge in the northwestern part of the area as discussed below. Based on the trend interpreted from the seismic data, the shale was inferred to trend southwest-northeast, parallel to the coast (Fig. 13A).

Houston Embayment: Survey #4

The main structural elements in this acreage are coast-parallel synthetic faults and erosional anticlines. In this survey, the top of the Vicksburg is less deformed than it is in survey #3. Here, the interpreted surface appears as a prominent detachment (decollement) surface, on top of which the lower Frio shale-prone strata appear to be structurally rotated (Figs. 6, 7B, and 8B). In map view, the surface is composed of two erosional anticlinal structures separated by a saddle and a down-to-the-southeast,

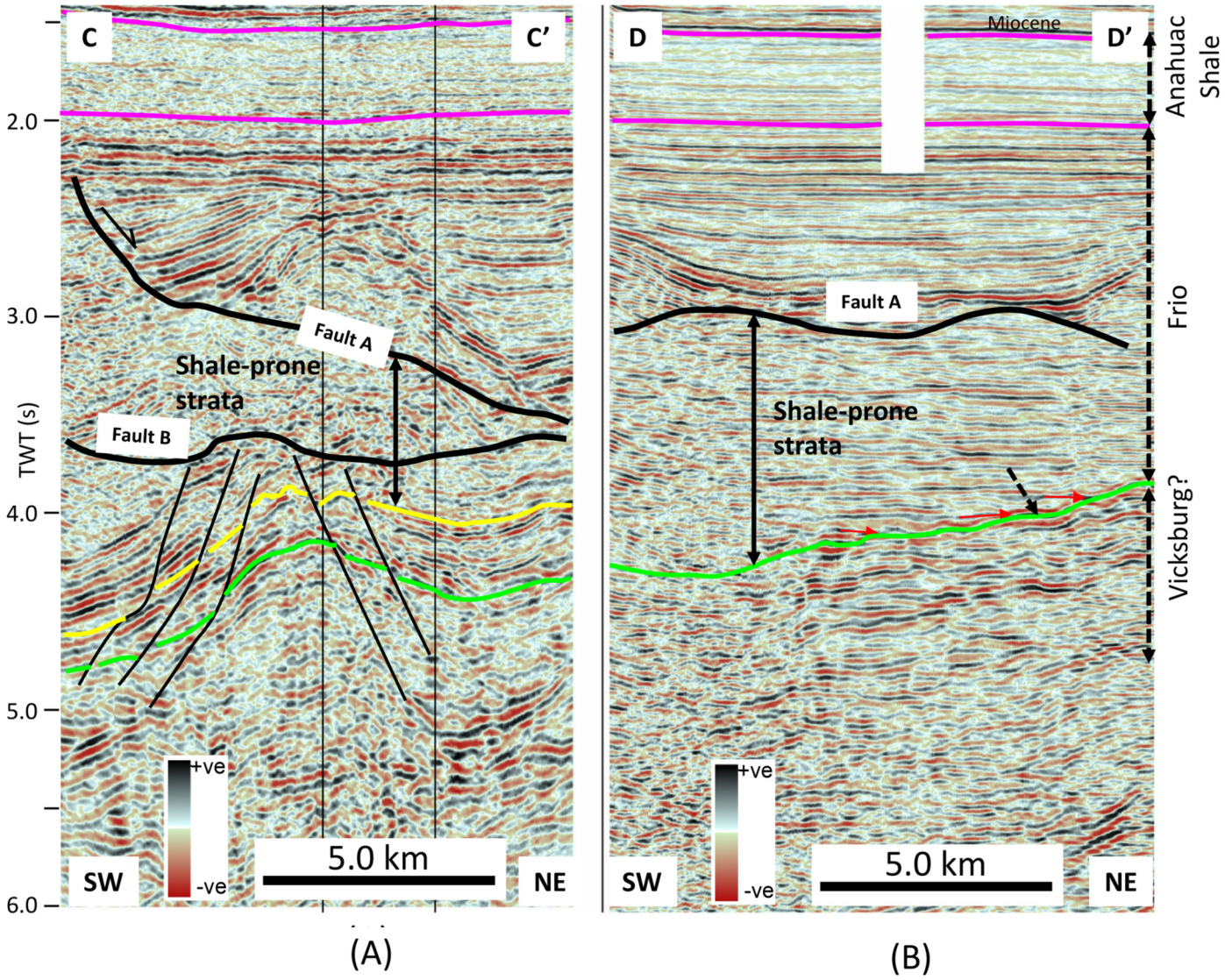

Figure 7. (A) Seismic line C–C' from survey #3 showing inferred top Vicksburg Formation (yellow horizon). Green horizon, 300 ms deeper than yellow, was mapped instead of yellow horizon (see text). Note lower Frio shale-prone sediments atop fault B and small-scale faults at flanks of shale-cored anticline. (B) Seismic line D–D' from survey # 4 showing interpreted top Vicksburg (green horizon). Note: Small red arrows = onlap direction of lower Frio sediments atop Vicksburg surface; and top and base Anahuac Shale shown in magenta color. Note unconformable nature of top Vicksburg horizon. 5 km = ~3.1 mi.

southwest-northeast trending fault U (Figs. 4 and 13B). The anticlinal structure is bounded on the southeast by the down-to-the-southeast synthetic fault (fault A), but the fault actually soles out along the surface (Figs. 6, 8, and 13B). Situated on top of the anticline are low-amplitude and high-frequency lower Frio sediments. Although well K did not test the entire lower Frio section, the penetrated section of it is shale-prone compared to the sandstone-rich upper Frio strata (Fig. 6) and may serve as a seal for possible hydrocarbons trapped by the anticline. However, there are some zones, such as the dashed magenta outline (Figs. 8B and 9B), within the lower Frio interval that may be sand-prone.

Although surveys #3 and #4 are separated by ~4 km (~2.5 mi), we observed that the erosional gully (coast-parallel valley) in survey #3 appears to continue into survey #4 (broad magenta arrow, Figs. 12A and 12B). Furthermore, the anticlinal structure in the southeastern part of survey #3 appears to correspond to the structural high in survey #4 (Figs. 12A and 12B); fault A in survey #3 also appears to correlate to fault A in survey #4. These correlations suggest that at the top of the Vicksburg, the structure in survey #4 is a continuation of the structural pattern in survey #3.

Evidence of Existence of Southwest-Northeast Trending Shale Ridge in Survey #3

The evidence confirming that the structure at the top Vicksburg strata in survey #3 is bounded by a southwest-northeast trending shale ridge in the north can be seen in well M located along line K–K' (red line, Fig. 14). In Figure 14A, the location of well M together with lines K–K' (red line), H–H' (green line), and the COCORP TX4 (dashed cyan line) are shown. Along line K–K', we interpreted the outlines of two shale-prone zones. Well M drilled into and bottomed in one of these shale-prone zones (Fig. 14B). Based on spontaneous potential and resistivity-log curves, the last 230 m (~750 ft) of the wellbore, starting from the blue arrow to the end of the well, is composed of very low

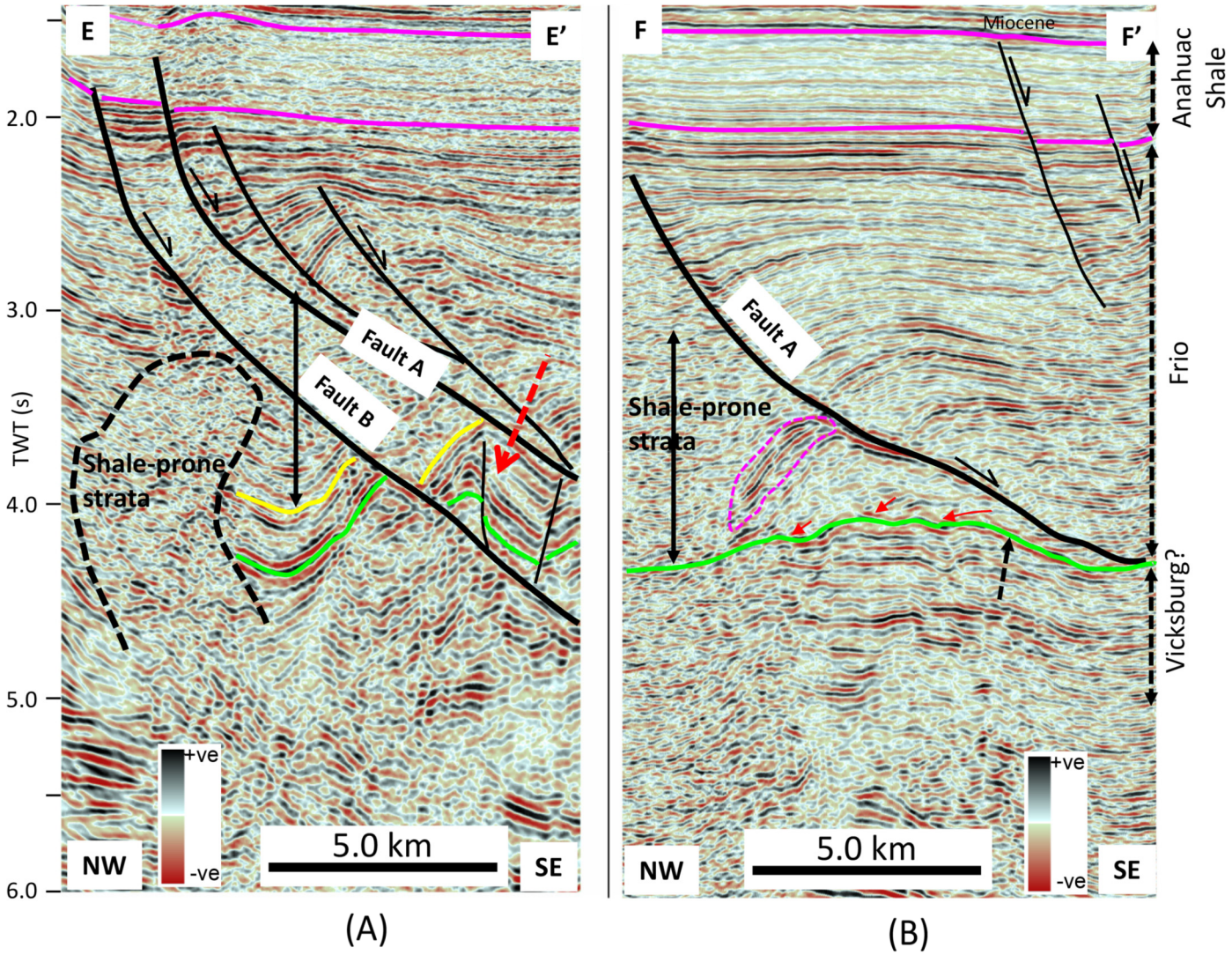

Figure 8. (A) Seismic lines E–E' from survey # 3 showing inferred top Vicksburg and interpreted shale diapir (dashed black outline). Green horizon, 300 ms deeper than yellow, was mapped instead of yellow horizon (see text). Note: Bold, dashed red arrow indicates folded and faulted block being rafted down fault plane. (B) Seismic lines F–F' from survey # 4 showing interpreted top Vicksburg Formation. Small red arrows = downlap direction of lower Frio sediments atop Vicksburg surface; and magenta horizons = top and base Anahuac Shale. Dashed magenta outline = possible sand-prone zone. 5 km = ~3.1 mi.

resistivity shale (Fig. 14B). From the blue arrow to the end of the well, formation resistivity decreases rapidly to almost zero ohm, while the conductivity increases rapidly to the maximum value of 2000 mmho (2000 millisiemens), suggesting that the shale-prone zone is overpressured (Fig. 14C).

Comparison of COCORP Line TX4 and 3D Seismic Line H–H'

In this section, we compare the COCORP TX4 line and line H–H' from our 3D survey #3 (Figs. 15A and 15B), whose locations are shown in Figure 14A. COCORP interpretation of TX4 shows the presence of a diapiric structure, albeit with a question mark that suggests uncertainty about the nature of the diapir (Fig. 15A). By comparing the interpretation of lines TX4 and H–H', we show that the questionable diapir in TX4 corresponds to the shale-prone zone delineated in H–H' (Fig. 14B). Note that line TX4 terminated within the diapir (Fig. 14A), where it almost merged with line H–H', and thus did not encounter the south-dipping flank of the diapir. Had line TX4 continued along line H–H' (Fig. 14A), it would have encountered the south-dipping flank of the diapir at the location where we have interpreted the shale-prone outline along line H–H'. However, the north-dipping flank of the shale-prone diapir along lines H–H' and K–K' was not defined because the lines did not extend to the northern part covered by line TX4 (Fig. 14). Had line H–H' continued along line TX4 (Fig. 14A), it would have found the north-dipping flank and would have been the same as the one encountered by line TX4. Based on these deductions, we interpret the diapir along line TX4 to be the same as the one along lines H–H' and K–K', which has been confirmed by well M to be composed of overpressured shale (Figs. 14B and 14C). Hence we interpret the south-dipping flank in TX4 and H–H' to be the same (Figs. 14 and 15). Therefore, we conclude that the questionable diapir in TX4 is an overpressured shale penetrated by well M, with the south-dipping flank being the same as the south-dipping flank along lines H–H' and K–K' (Fig. 14).

We interpret the age of the diapir in the Rio Grande Embayment (survey #2) to be late Eocene–early Oligocene, when the uprising shale terminated just about the top of the Vicksburg—and in some cases penetrated a little bit into the lower Frio

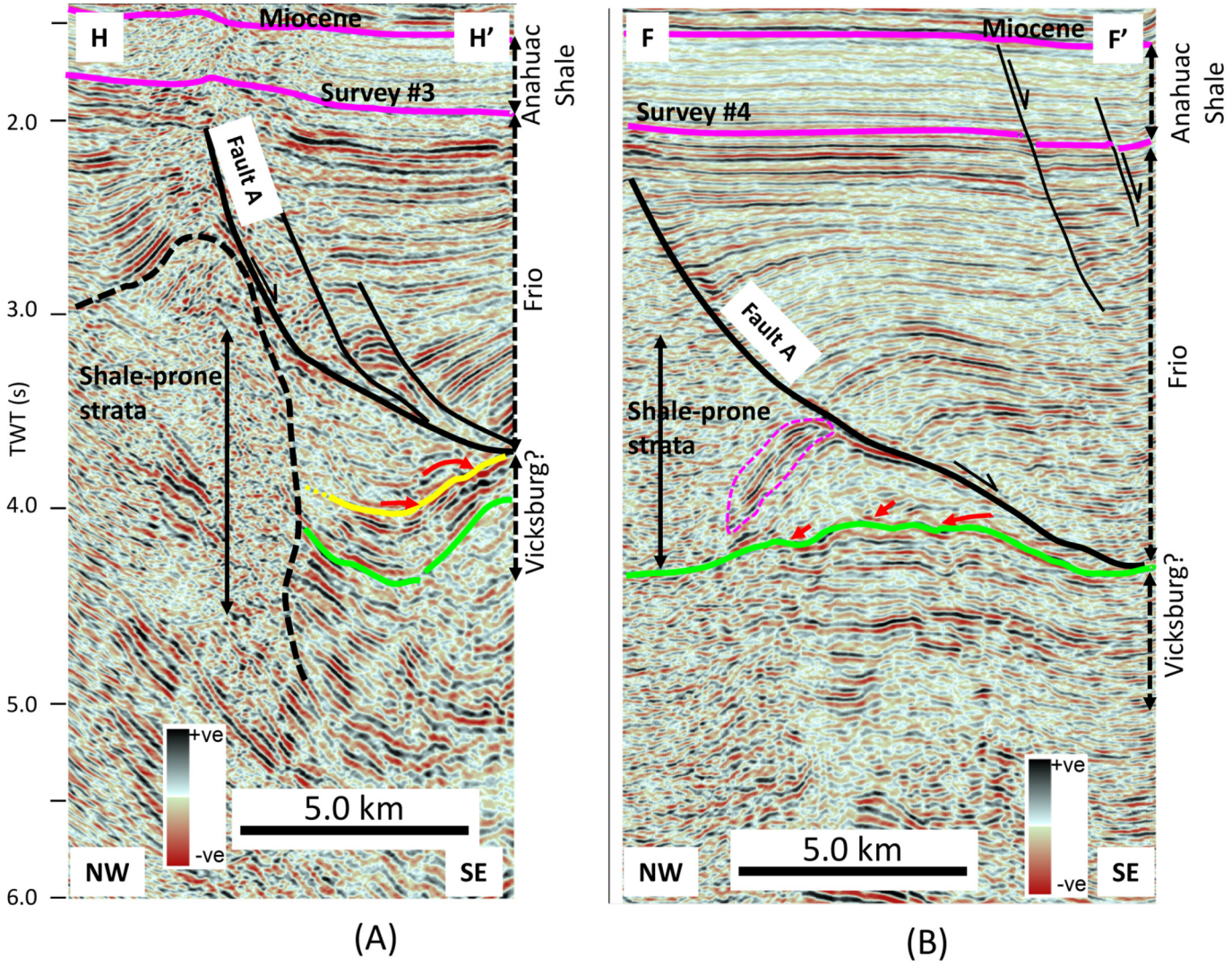

Figure 9. (A) Seismic lines H–H' from survey # 3 showing inferred top Vicksburg and interpreted shale diapir (dashed black outline). Green horizon, 300 ms deeper than yellow, was mapped instead of yellow horizon (see text). Note unconformable nature of yellow horizon. (B) Seismic lines F–F' from survey # 4 showing interpreted top Vicksburg Formation. In (A) and (B), small red arrows = downlap direction of lower Frio sediments atop Vicksburg surface; and magenta horizons = top and base Anahuac Shale. Dashed magenta outline = possible sand-prone zone. 5 km = ~3.1 mi.

(Fig. 12). As noted by Ogiesoba and Hernandez (2015), the diapir stopped rising when the pressure within the overpressured shale had substantially bled off because both the small- and large-scale faults that served as pressure-release valves cut into the diapirs. In the Houston Embayment, because the diapir continued into the lower and middle Frio (Figs. 9 and 15), we interpret the age of the diapir in this basin to be early-middle Oligocene. Although the possible causative mechanisms of the shale diapirs have already been discussed by Ogiesoba and Hernandez (2015), we note that while the possible cause of diapirism in the Rio Grande may be due to a combination of vertical loading and local lateral compression of the rapidly deposited sediments, in the Houston Embayment the possible causative mechanism may be due to vertical loading only.

3D Visualization of Mapped Surfaces, Shale Ridges, and Diapirs

This section presents 3D visualization of the mapped surfaces in surveys #1 through #4 (Fig. 16). Figure 16 clearly shows the curvilinear faults in survey #1 and the curvilinear appearance of SB 1 in survey #2. These features are better displayed in Figure 17, where the stepping fault pattern of the curvilinear faults in survey #1 and the nature of the subbasins, shale ridges, and diapirs in survey #2 are clearly highlighted. A more accentuated view of the structures identified in surveys #3 and #4 are shown in Figures 18A and 18B, respectively. Figure 18A shows without any doubt a high-rise southwest-northeast trending shale ridge penetrated by well M to the north and bounding a southwest-northeast trending deep valley. In Figure 18B, the erosional anticlines in survey #4 are prominently differentiated from the synclines. Although more seismic data would be required to firm up the areal extent of these anticlines, they nevertheless constitute potential hydrocarbon targets.

HYDROCARBON POTENTIAL

This section focuses on the hydrocarbon potential of the Vicksburg within the study area by examining the structural closures, caprock, and possible sandstone richness/distribution in each survey area. In survey #1, the curvilinear anticlines are strongly defined and, as revealed by well J (Fig. 19), the struc-

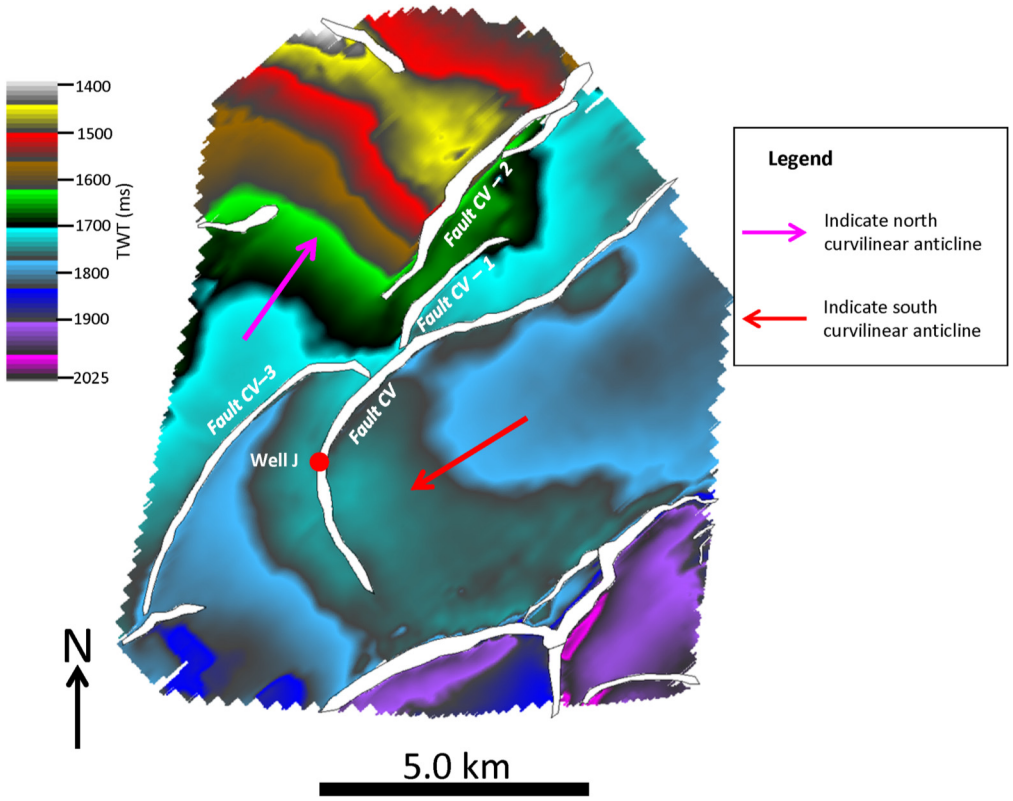

Figure 10. Map of top Vicksburg Formation in survey #1 showing faulted northwest-southeast trending curvilinear anticline. Dominant structural styles are down-to-southeast synthetic growth faults. 5 km = ~3.1 mi.

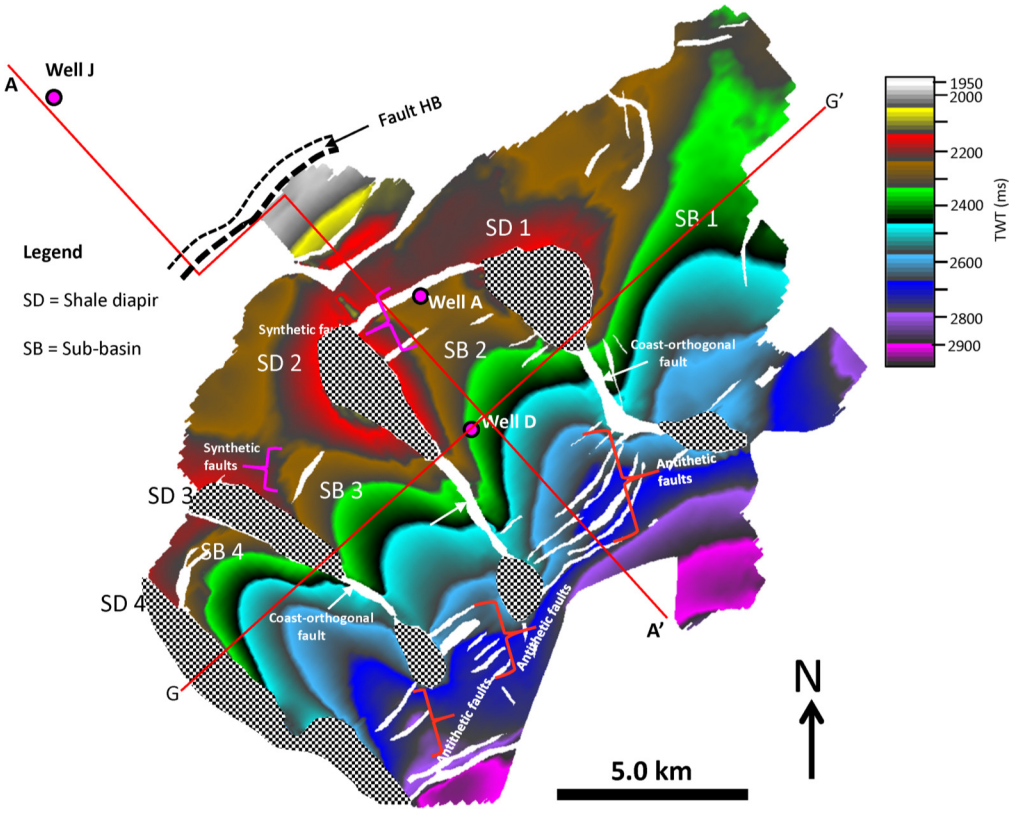

Figure 11. Map of top Vicksburg Formation in survey #2 showing four coast-orthogonal shale ridges, four coast-orthogonal shale subbasins, and three coast-orthogonal faults, as well as coast-parallel synthetic and antithetic faults. 5 km = ~3.1 mi.

tures at the Vicksburg surface have a gross reservoir sandstone thickness of about 30 m (~100 ft). However, the caprock integrity is in question. As shown by well J (Fig. 19), the top of the Vicksburg is in the middle of a sand-prone interval, suggesting that the unconformity surface separating the upper Vicksburg and the lower Frio is a sand-on-sand contact. The placement of the top Vicksburg surface at this depth (~2130 m [~6980 ft]) is supported by paleoanalysis. The surface is identified by *Lanter-*

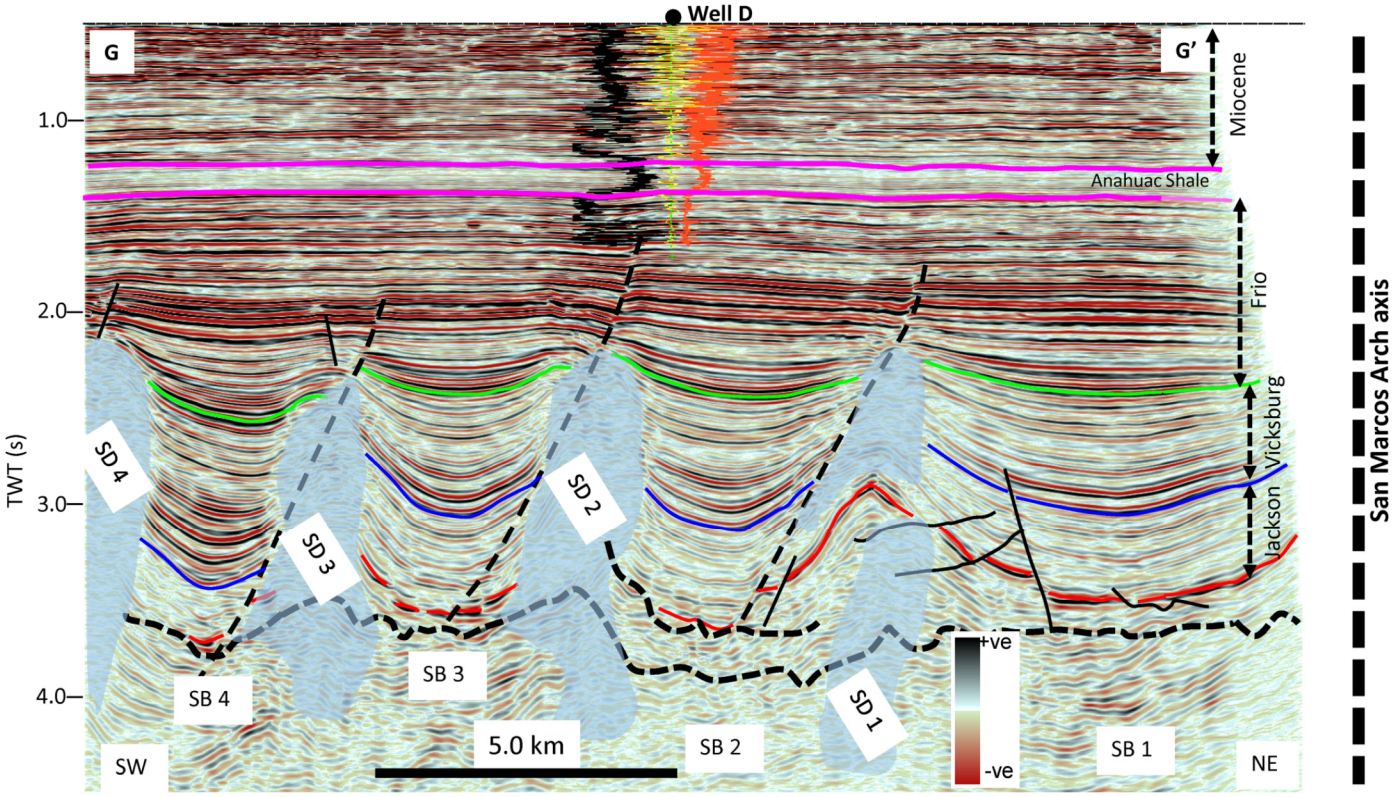

Figure 12. Seismic lines G–G' from survey # 4 through well D showing top Vicksburg (green horizon), top Jackson (blue horizon), top Frio (lower magenta horizon), and top Anahuac Shale (upper magenta horizon). Note alternating shale diapirs (SD 1 to SD 4) and subbasins (SB 1 to SB 4). Approximate location of San Marcos Arch axis is shown on right side of this figure (see actual location in Figure 1). Red horizon = near base Jackson. Black log curve = gamma ray log; and red log curve = sonic log. 5 km = ~3.1 mi.

nithus minutus (31.10 Ma) and *Rhabdosphaera tenuis* (31.70 Ma) nannofossils that are characteristic of the upper Vicksburg, whereas the lower Frio is characterized by *Helicosphaera wilcoxonii* (30.0 Ma) and *Helicosphaera compacta* (30.0 Ma) nannofossils. In Figure 19, the last 100 m (~300 ft) of the lower Frio shale that caps the curvilinear anticlines is composed of interbedded sandstones and shale beds. The thickness of each shale bed ranges from about 6–20 m (~20–60 ft), while the thickness of sandstone beds ranges from about 3–12 m (~10–40 ft). Because this lower Frio shale is not composed of 100 percent shale, it cannot be regarded as a good caprock with good sealing properties. Thus, the lack of hydrocarbons in well J can be attributed to either the poor sealing properties of the caprock overlying the curvilinear anticlines at this location or because it was drilled too far downdip of the structural crest and potentially outside of closure as suggested by Figure 5, or due to a combination of both.

In the survey #2 area, the structures are essentially fault closures with many crestal faults. Because this area is more distally located basinward, the caprock could be shalier than in survey #1. However, the presence of many crestal faults and the poor rollover character reduced the hydrocarbon trapping potential of these fault closures.

In contrast, as evidenced by the bottom part of well M (that is, the last 230 m [~750 ft] of the wellbore), the lower Frio shale capping the faulted erosional anticlines in survey areas #3 and #4 is composed of almost 100 percent continuous shale (Fig. 14C). These sediments are characterized by low-amplitude and high-frequency events. These events extend from the bottom of the borehole to the top of the faulted erosional anticlines—from ~3.0 –4.1 s (Fig. 14B). Because these seismic events are very similar to those that characterize the bottom part of well M suggests that the interval from 3.0–4.1 s would be mostly shale, albeit there are some zones such as the dashed magenta outline that may be sand-prone (Figs. 8B and 9B). Therefore, the caprock overlying the faulted erosional anticlines can be regarded as very competent with good sealing properties.

In these two survey areas, the main concern with respect to hydrocarbon trapping potential is whether there will be reservoir sandstones. To address this issue, we extracted sweetness and instantaneous frequency attributes. These two attributes have been shown to be very effective in the identification of sandstone-rich zones in shale-dominated depositional environments (Ogiesoba, 2017; Ogiesoba et al., 2018). The relationship between sandstone richness and the sweetness attribute shows that the sweetness value increases as sandstone richness increases (Ogiesoba, 2017). In addition, instantaneous frequency values increase as shale content increases; that is, low values of instantaneous frequency suggest an increase in sandstone richness (Robertson and Fisher, 1988; Taner, 2003; Ogiesoba et al., 2018). On the basis of these deductions, we extracted sweetness and instantaneous frequency along the Vicksburg surface and identified sandstone-rich zones in surveys #3 and #4. In Figure 20, we show the sweetness attribute map that was extracted in these two surveys. As can be seen in Figure 20A, the high sweetness values (green to red to yellow color) indicative of sandstone-rich zones are enclosed by the dotted-black outline. On transferring this outline onto the instantaneous frequency map (Fig. 20B), we find that the outline is coincident with the outline of the low-frequency zone. Values within the low-frequency zone range from ~5–15 Hz (magenta to deep blue, Fig. 20B), whereas values within the high-frequency (shale-rich) zones range from ~20–45 Hz (cyan to yellow, Fig. 20B). By transferring sandstone-rich

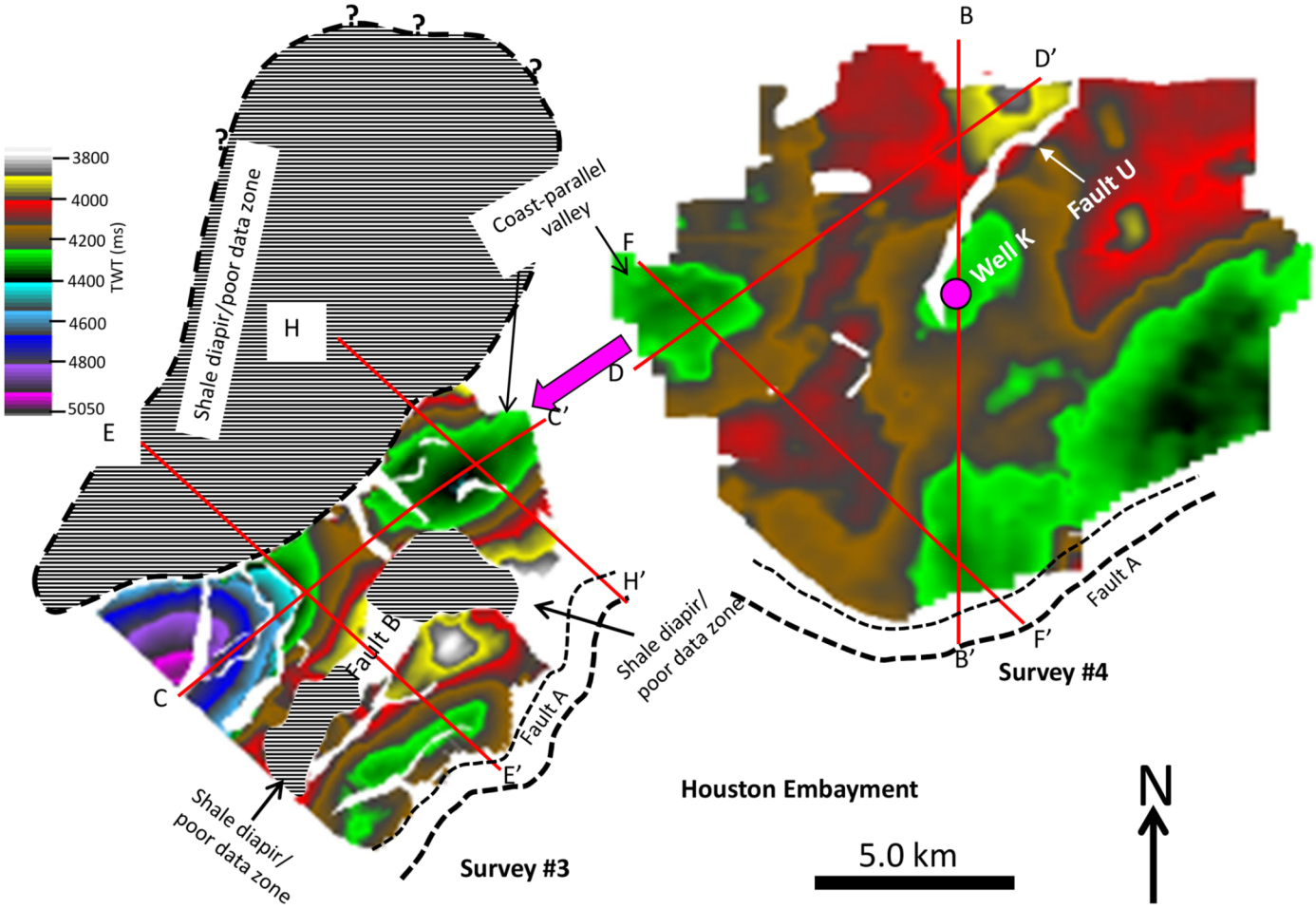

Figure 13. (A) Map of top Vicksburg Formation in survey #3 showing southwest-northeast trending faulted anticline, southwest-northeast trending interpreted shale diapir/poor data zone, minor antithetic faults, and minor coast-orthogonal faults. (B) Map of top Vicksburg Formation in survey #4 showing three lines of sections discussed in text and erosional anticline having two culminations. Note question marks along dashed black line suggesting uncertainty in diapir boundary. 5 km = ~3.1 mi.

outlines on the structure map, it can be seen that the structurally high areas fall within the sandstone-rich zones (Figs. 21A and 21B). In the southwestern part of survey #4, the sandstone-rich outline coincides with the closing contour (4200 ms, yellow outline). It appears that almost all the erosional highs in survey #4 are sandstone-rich, suggesting that the highs are remnant sandstone beds resistant to erosion. We consider these erosional highs to be prospective because the structures have both vertical and lateral seal. However, in survey #3, apart from the central structural fault closure to the northwest along line E–E', all other highs are shale-prone. Some other areas that appear to be sandstone-rich, such as in the southeast along line E–E', are in a low.

SUMMARY AND CONCLUSIONS

The results of the above investigations are summarized in Figures 16 and 22 (2D version of Figure 16). In the Rio Grande Embayment, the surface of detachment occurs just below the base of the Jackson Group (Fig. 5); in the Houston Embayment, the top of the Vicksburg Group is interpreted to be the detachment surface.

In the Rio Grande Embayment, in addition to the coast-parallel synthetic and antithetic faults, the pattern of deformation includes prominent alternating coast-orthogonal shale ridges, subbasins, and coast-orthogonal faults that suggest local lateral compression and vertical loading. Furthermore, structural elements also exhibit northwest-southeast trending curvilinear anticlines. In the Houston Embayment, the dominant structural elements are coast-parallel synthetic faults and coast-parallel shale ridges.

Deformation in the Houston Embayment is more severe than in the Rio Grande Embayment and increases with nearness to the axis of the San Marcos Arch. In the Rio Grande Embayment, the subsea elevation of the top of the Vicksburg Group ranges from a seismic two-way time of ~1380–3000 ms (~1550–3380 m [~5085–11,100 ft]); in the Houston Embayment, it ranges from ~3770–5050 ms (~4600–5850 m [~15,100–19,200 ft]).

Based on the map at the top of the Vicksburg in the vicinity of the San Marcos Arch, we conclude the following: (1) although the prevailing mechanism of deformation during the deposition of the Eocene (Jackson Group) and Oligocene (Vicksburg Group) in the Rio Grande and Houston embayments was extensional tectonics, stratal deformational patterns are different in each basin; (2) the Houston Embayment is deeper than the Rio Grande; (3) the geometry of the San Marcos Arch must have influenced the shape and depths of the basins and, thus, the stratal deformational patterns; and (4) on the basis of sweetness and instantaneous frequency attributes, the remnant erosional anticlinal structure within the Houston Embayment, which is capped by more than 1000 m (~3200 ft) thick shale and has a vertical closure of ~180–250 m (~590–820 ft) in survey #4, constitutes a potential hydrocarbon prospect. However, more 3D seismic data

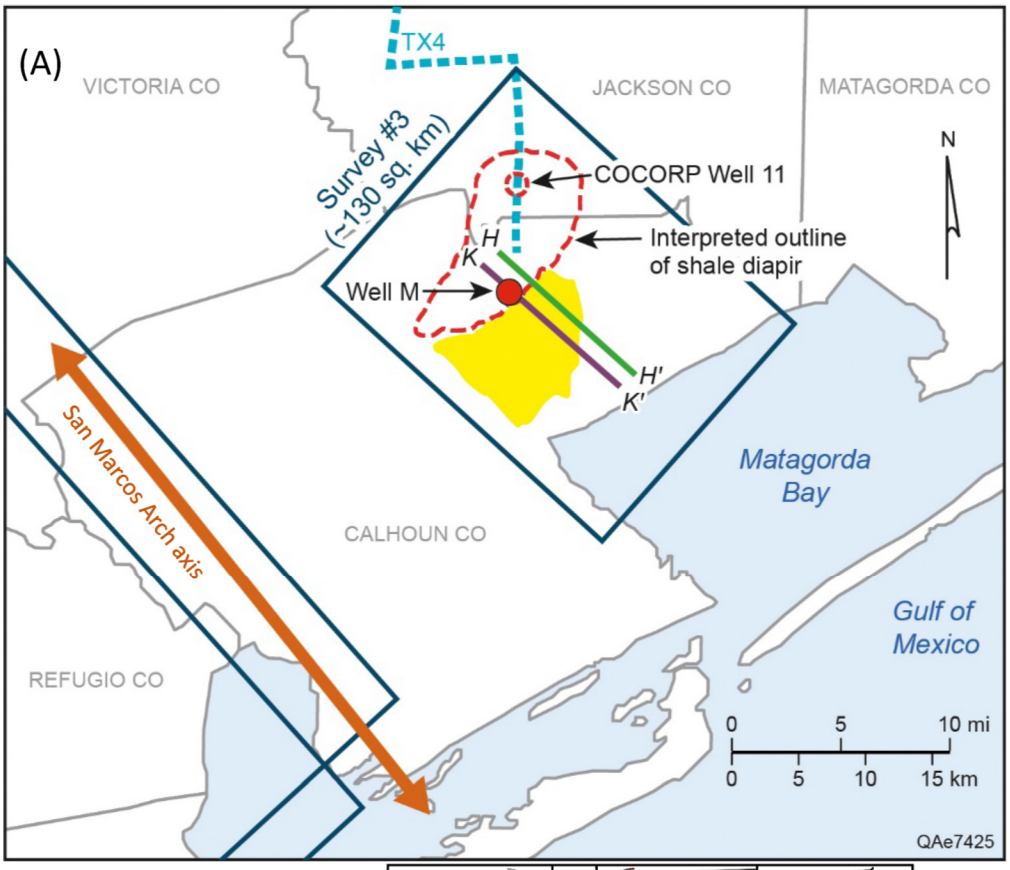

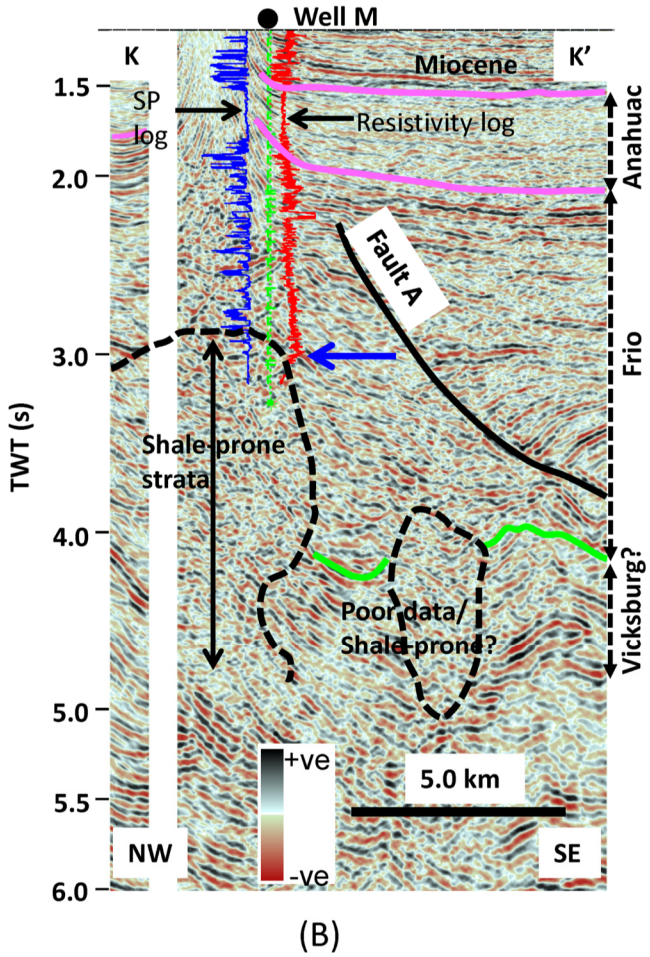

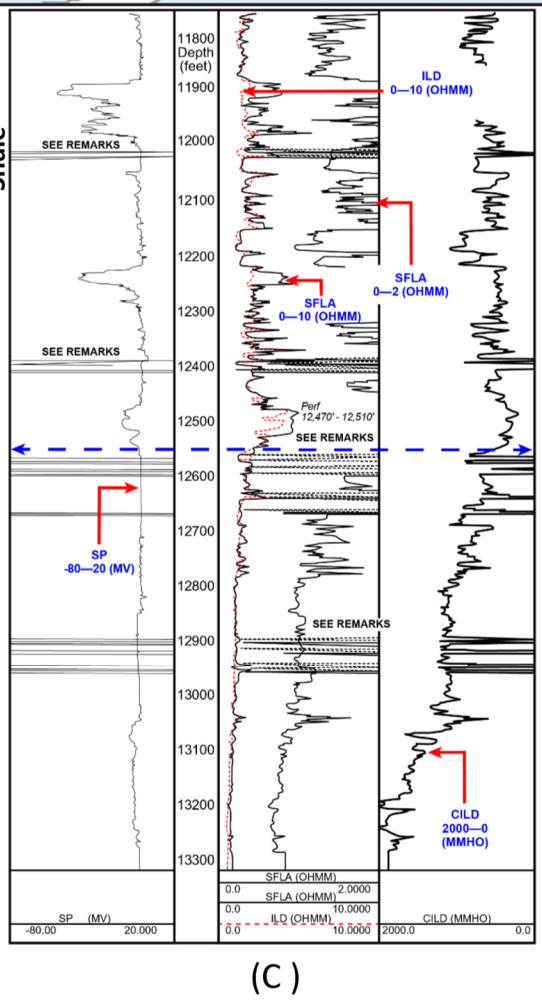

Figure 14. (A) Base map showing locations of well M, lines H–H' (green), K–K' (magenta), interpreted outline of shale diapir (dashed red line), location of COCORP well 11, and COCORP TX4 (cyan). (B) Line K–K' through well M. Note that well M bottomed within shale-prone diapir. 5 km = ~3.1 mi. (C) Log responses in well M. Note rapid decrease of resistivity (ILD) from the dashed blue, double-headed arrow to near zero ohm-m at end of well, and rapid increase of conductivity (CILD), the double-headed arrow to 2000 mmho (2000 millisiemens) at end of well. Note: "See Remarks" indicates tight hole where drilling-tool string is pulling intermittently, induction and spontaneous potential curves appear to fail, and caliper is being closed/opened to free the tool—suggesting sticky and swelling shale zones. 100 ft = ~30.5 m.

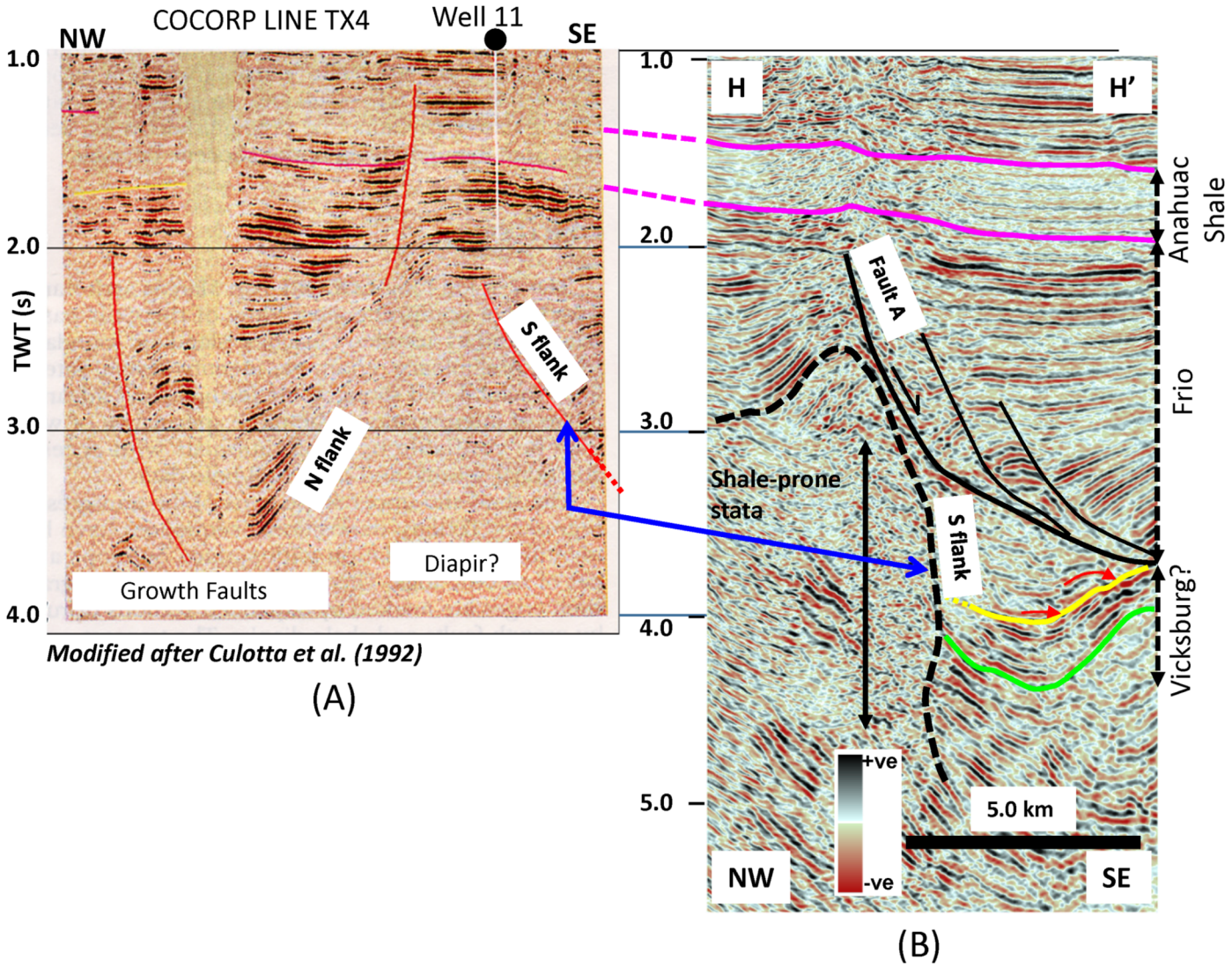

Figure 15. Comparison between (A) COCORP interpreted line TX4 (modified after Culotta et al., 1992) and (B) 3D line H–H'. Note that diapir with a question mark in TX4 corresponds to shale-prone diapir identified in H–H'. See text for more details. 5 km = ~3.1 mi.

are needed to determine the full areal extent of these structures to the northeast.

ACKNOWLEDGMENTS

The research was funded by the STARR (State of Texas Advanced Oil and Gas Resource Recovery Program) and the Deep Shelf Gas Consortium at the Bureau of Economic Geology, The University of Texas at Austin. We thank Landmark Graphics Corp. for providing the software used in this study. We also thank T. C. Oil Company, Neumin Oil and Gas Exploration, and Brigham Oil Company for supplying 3D seismic data. Publication authorized by the Director, Bureau of Economic Geology.

REFERENCES CITED

Coleman, J., and W. E. Galloway, 1990, Petroleum geology of the Vicksburg Formation, Texas: Gulf Coast Association of Geological Societies Transactions, v. 40, p. 119–130, <http://archives.datapages.com/data/gcags/data/040/040001/pdfs/0119.pdf>.

Culotta, R., T. Latham, M. Sydow, J. Oliver, L. Brown, and S. Kaufman, 1992, Deep structures of the Texas Gulf passive margins and its Ouachita-Precambrian basement: Results of the COCORP San Marcos Arch survey: American Association of Petroleum Geologists Bulletin, v. 76, p. 270–283, <http://archives.datapages.com/data/bulletns/1992-93/images/pg/00760002/0000/02700.pdf>.

Galloway, W. E., D. K. Hobday, and K. Magara, 1982, Frio formation of the Texas Gulf Coast Basin—Depositional systems, structural framework, and hydrocarbon origin, migration, distribution, and exploration potential: Bureau of Economic Geology Report of Investigations 122, Austin, Texas, 78 p., <https://store.beg.utexas.edu/reports-of-investigations/1085-ri0122.html>.

Galloway, W. E., P. E. Ganey-Curry, X. Li, and R. T. Buffler, 2000, Cenozoic depositional history of the Gulf of Mexico Basin: American Association of Petroleum Geologists Bulletin, v. 84, p. 1743–1774, <http://archives.datapages.com/data/bulletns/ 2000/11nov/1743/images/00_1743.pdf>.

Halbouty, M. T., 1966, Stratigraphic-trap possibilities in Upper Jurassic rocks, San Marcos Arch, Texas: American Association of Petroleum Geologists Bulletin, v. 50, p. 3–24, <http://archives.datapages.com/data/bulletns/1965-67/images/pg/00500001/0000/00030.pdf>.

Henry, C. D., and F. W. McDowell, 1986, Geochronology of magmatism in the Tertiary volcanic field, Trans-Pecos Texas, *in* J. G. Price, C. D. Henry, D. F. Parker, and D. S. Barker, eds.,

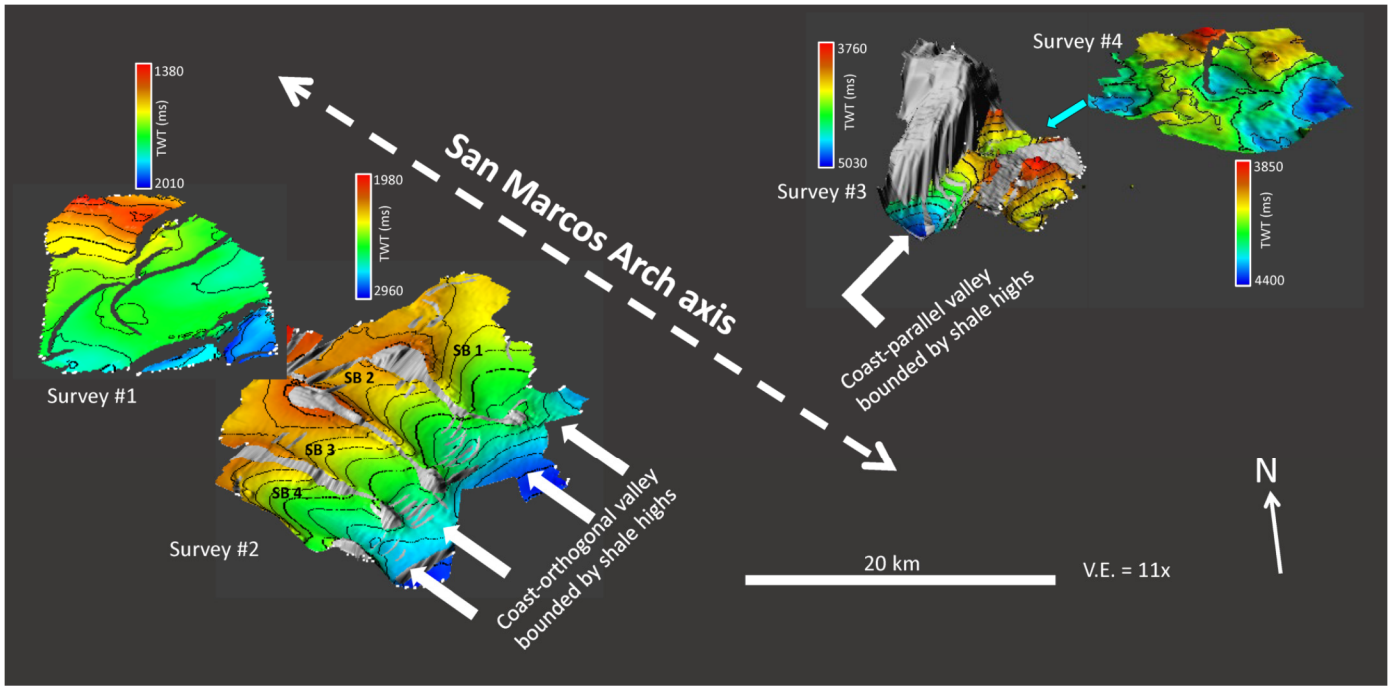

Figure 16. 3D display of top Vicksburg map in surveys #1 through #4. Note enhanced curvilinear faults in survey #1 and coast-orthogonal faults, subbasins, shale ridges, and curvilinear subbasin SB 1 in survey #2. 20 km = ~12.4 mi.

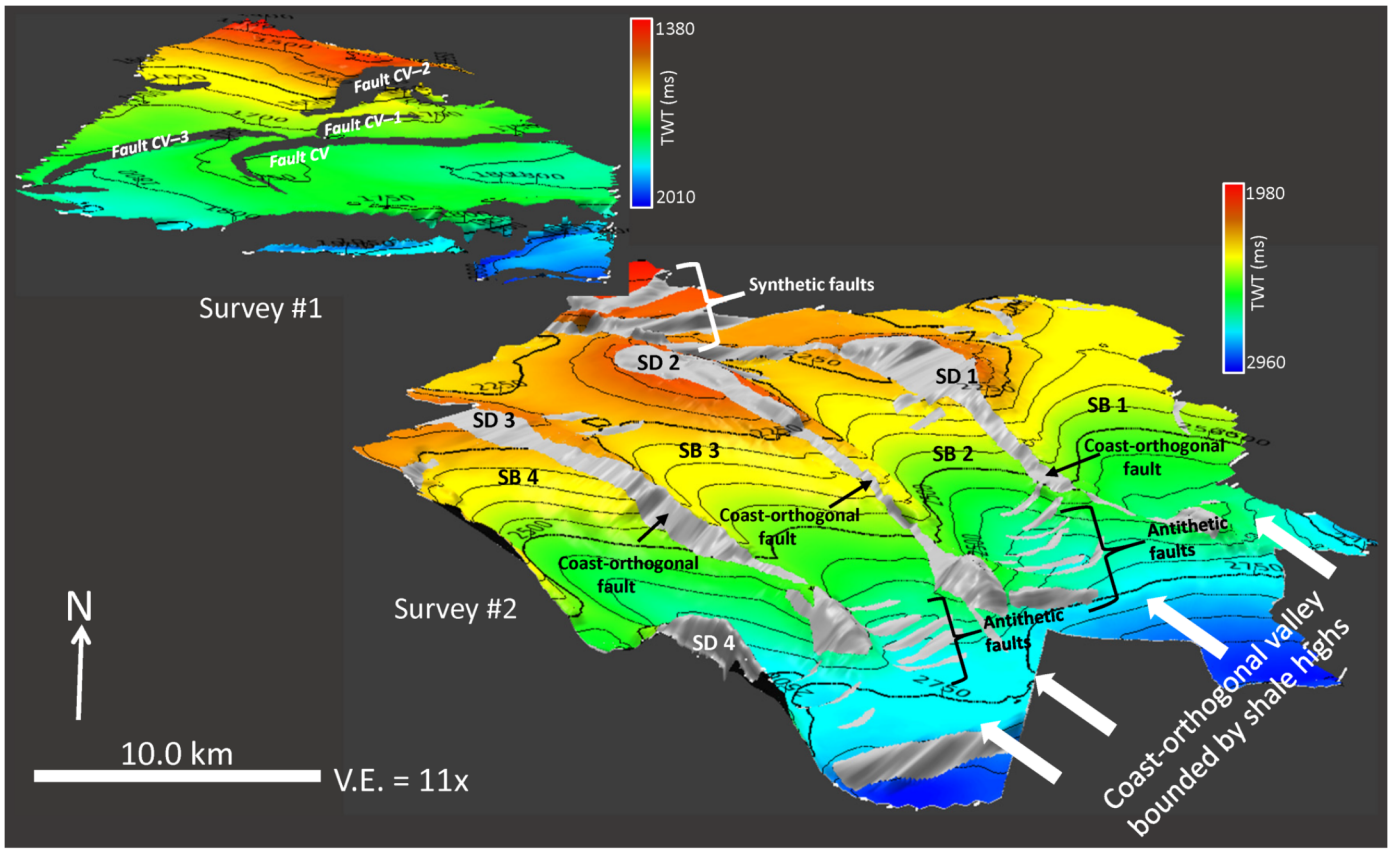

Figure 17. 3D display of top Vicksburg map in surveys #1 and #2. Note accentuated curvilinear faults in survey #1 and accentuated coast-orthogonal faults, subbasins, shale ridges, and curvilinear subbasin SB 1 in survey #2. 10 km = ~6.2 mi.

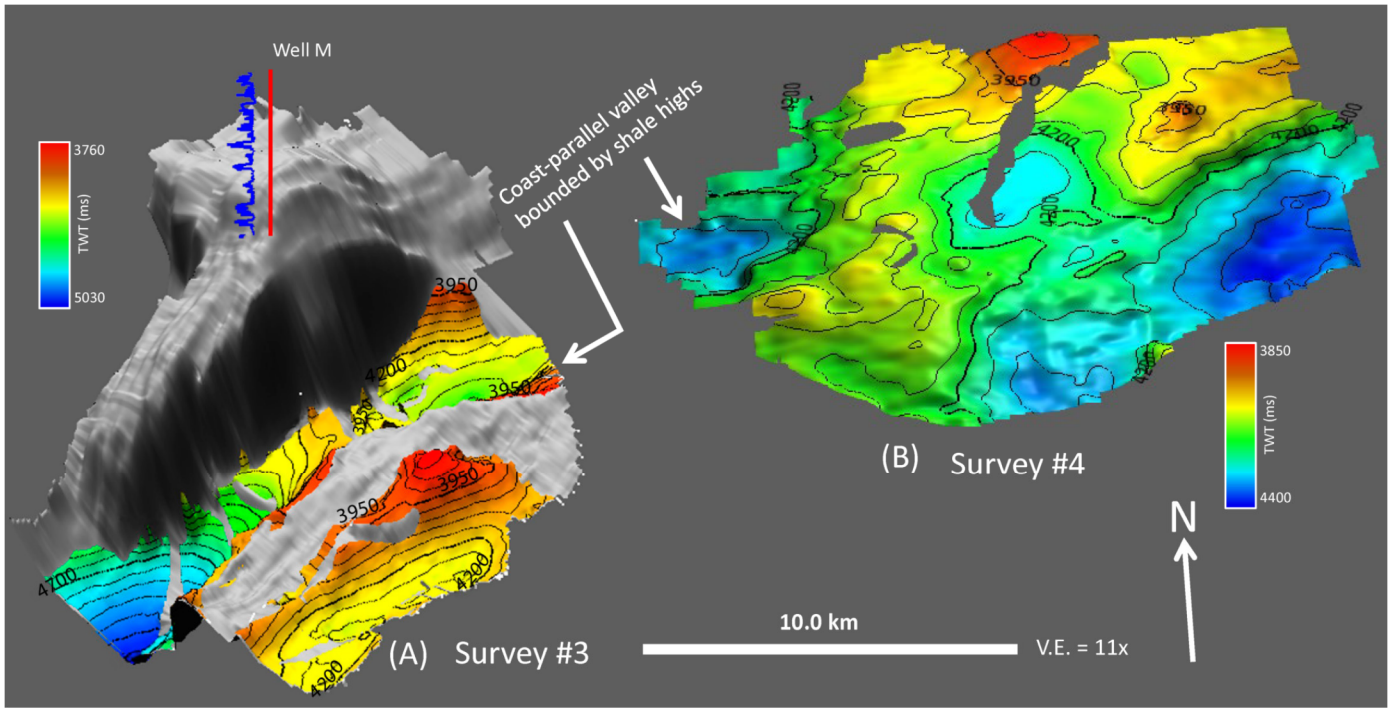

Figure 18. 3D display of top Vicksburg map in (A) survey #3 showing well M penetration into shale mass (note accentuated coast-parallel shale ridges and valleys) and (B) survey #4. Note accentuated erosional anticlines. Displayed log curve in well M = spontaneous potential log. 10 km = ~6.2 mi.

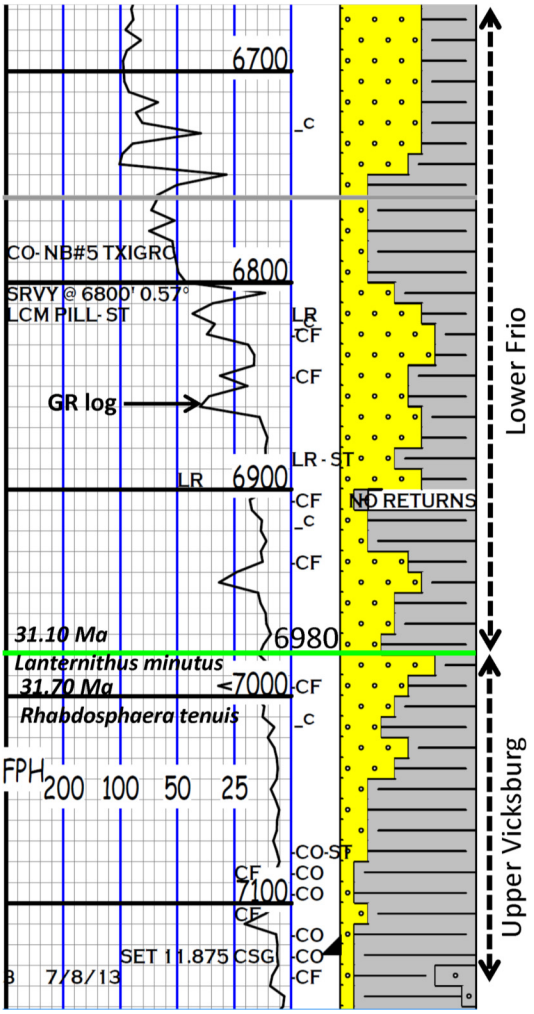

Figure 19. Gamma ray log (GR log) from well J showing depth intervals between ~2040–2180 m (~6700–7150 ft) and depths to top Vicksburg (~2130 m [~6980 ft]). Note Frio strata overlying top Vicksburg are composed of sandstone and shale beds, suggesting shales with poor sealing properties—weak caprock. 100 ft = ~30.5 m.

Igneous geology of Trans-Pecos Texas—Field trip guide and research articles: Bureau of Economic Geology Guidebook 23, Austin, Texas, p. 99–122, <https://store.beg.utexas.edu/guidebooks/377-gb0023.html>.

Laubach, S. E., and M. L. W. Jackson, 1990, Origin of the arches in the northwestern Gulf of Mexico Basin: Geology, v. 18, p. 595–598, <https://doi.org/10.1130/0091-7613(1990)018<0595: OOAITN>2.3.CO; 2>.

Murray, G. E., 1961, Geology of the Atlantic and Gulf Coastal Province of North America: Harper, New York, 692 p., <https://doi.org/10.1126/science.135.3508.1057>.

Ogiesoba, O. C., and U. Hammes, 2012, Seismic interpretation of mass-transport deposits within the upper Oligocene Frio Formation, South Texas Gulf Coast: American Association of Petroleum Geologists Bulletin, v. 96, p. 845–868, <https://doi.org/10.1306/09191110205>.

Ogiesoba, O. C., and R. Hernandez, 2015, Diapiric shale and coast-perpendicular, fault-related subbasins, South Texas Gulf Coast: Interpretation, v. 3, p. T43–T56, <https://doi.org/10.1190/INT-2014-0016.1>.

Ogiesoba, O. C., 2017, Application of thin-bed indicator and sweetness attribute in the evaluation of sediment composition and depositional geometry in coast-perpendicular subbasins, South Texas Gulf Coast: Interpretation, v. 5, p. T87–T105, <https://doi.org/10.1190/INT-2015-0213.1>.

Ogiesoba, O. C., W. A. Ambrose, and R. G. Loucks, 2018, Application of instantaneous-frequency attribute and gamma ray wireline logs in the delineation of lithology in Serbin Field, southeast Texas: A case study: Interpretation, v. 6, p. T1023–T1043, <https://doi.org/10.1190/INT-2018-0067.1>.

Robertson, J. D., and D. A. Fisher, 1988, Complex seismic trace attributes: The Leading Edge, v. 7, p. 22–26, <https://doi.org/10.1190/1.1439517>.

Taner, M. T., 2003, Attributes revisited, <http://www.rocksolidimages.com/attributes-revisited/>.

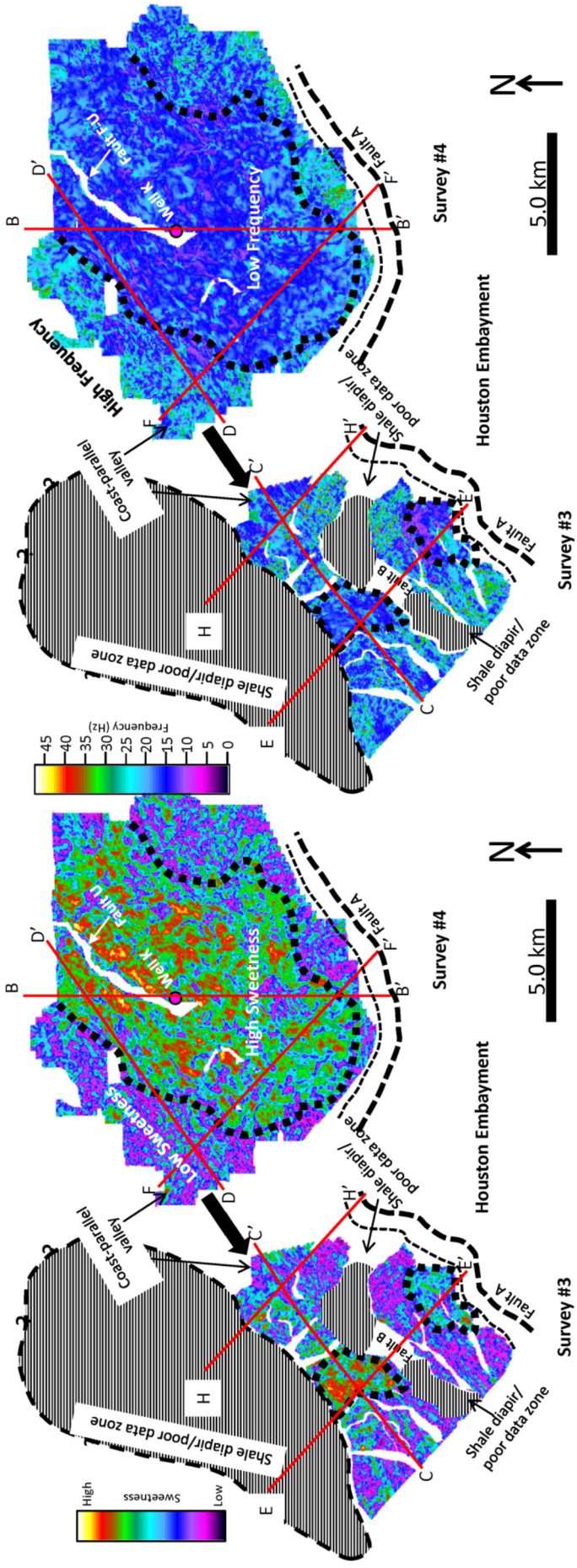

Figure 20. Maps showing extracted attributes along top Vicksburg horizon in surveys #3 and #4. (A) Sweetness map and (B) instantaneous frequency map. Note southwest-northeast trending shale diapir. Note question marks along dashed black line suggesting uncertainty in diapir boundary. 5 km = ~3.1 mi.

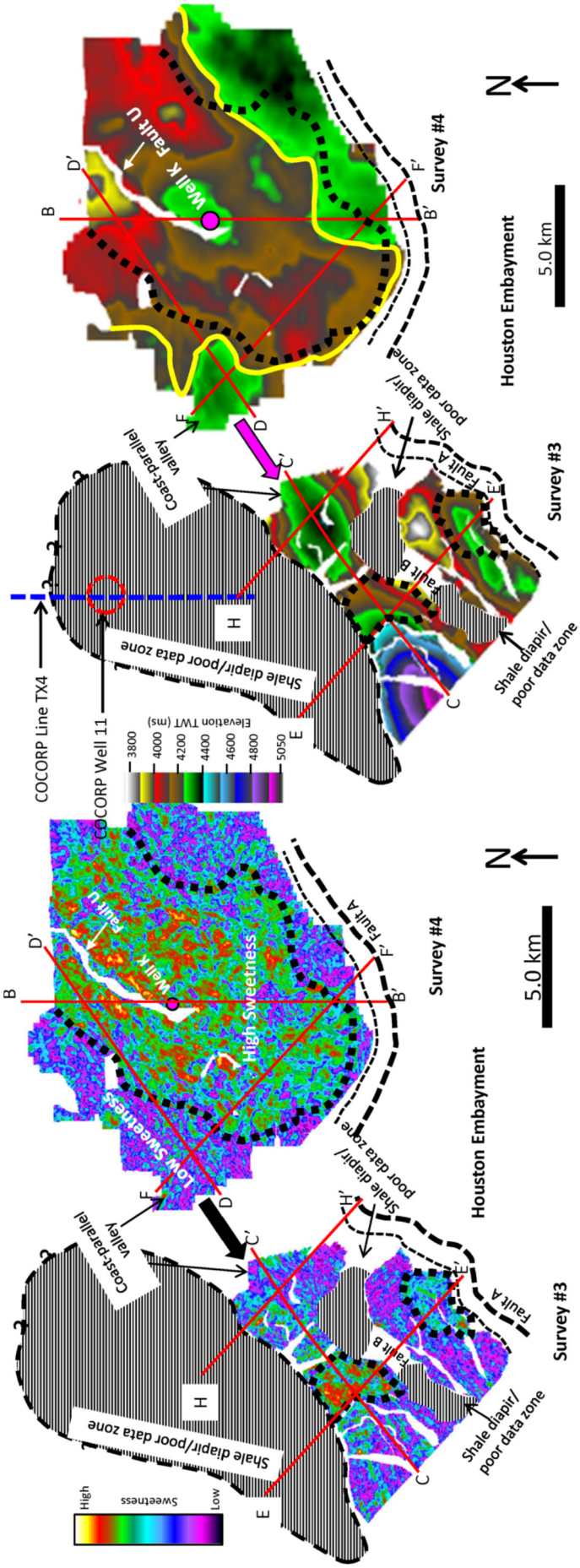

Figure 21. Maps showing outlines of high sweetness value areas (dotted black lines) overlain on top Vicksburg structure map in surveys #3 and #4. Note that high sweetness values suggest sandstone-rich zones. Yellow line = ~1280 m (~4200 ft) contour line. Note southwest-northeast trending shale diapir. Note question marks along dashed black line suggesting uncertainty in diapir boundary. 5 km = ~3.1 mi.

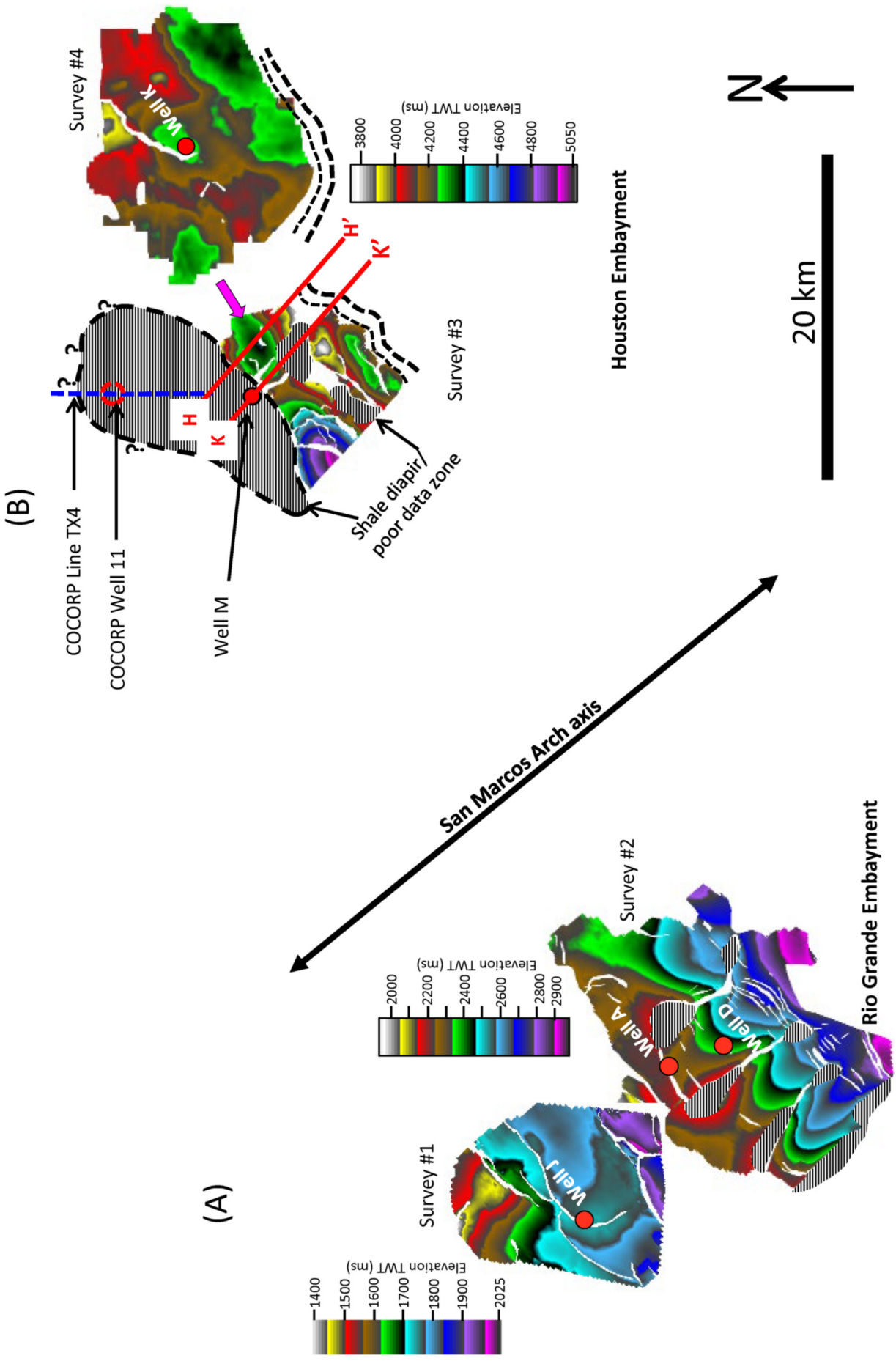

Figure 22. Map of top Vicksburg in surveys #1 through #4 showing location of San Marcos Arch axis and combined maps in surveys #1 and #2. Note that combined top Vicksburg map in surveys #1 and #2 have different color values, ranging from 1380 to ~2025 ms and from 1980 to 2980 ms, respectively. Maps in surveys #3 and #4 have the same color values, ranging from 3770 to 5050 ms. Note southwest-northeast trending shale diapir, a segment of COCORP line TX4, and COCORP well 11. Note question marks along dashed black line suggesting uncertainty in diapir boundary. 20 km = ~12.4 mi.